Cross-disorder comparison of Brain Structures among 4,842 Individuals with Mental Disorders and Controls utilizing Danish population-based Clinical MRI Scans

Authors: Stefano Cerri, PhD[1,2], Vardan Nersesjan, MD, PhD[1], Kiril Vadimovic Klein, MSc[2], Enric Cristòbal Cóppulo, MSc[1], Sebastian Nørgaard Llambias, MSc[2], Mostafa Mehdipour Ghazi, PhD[2], Mads Nielsen, PhD[2, *], Michael Eriksen Benros, MD, PhD[1,3, *]

Affiliations:

1: Copenhagen Research Centre for Biological and Precision Psychiatry, Mental Health Centre Copenhagen, Copenhagen University Hospital, Hellerup, Denmark.

2: Department of Computer Science, University of Copenhagen, Copenhagen, Denmark

3: Department of Clinical Medicine, Faculty of Health and Medical Sciences, University of Copenhagen, Copenhagen, Denmark

* shared last authorship

Correspondence:

- Stefano Cerri, PhD; stefano.cerri@regionh.dk,
Gentofte Hospitalsvej 19, st., 2900, Hellerup, Denmark, +45 50345029
- Professor Michael E. Benros, MD, PhD; benros@dadlnet.dk,
Gentofte Hospitalsvej 19, st., 2900, Hellerup, Denmark, +45 26255239

Keywords: mental disorders, brain morphology**,** observational studies, electronic health records, clinical cohort

ABSTRACT:

Large-scale mega-analyses of worldwide combined Magnetic Resonance Imaging (MRI) studies have demonstrated brain differences between individuals with mental disorders and controls. However, the potential of large-scale observational studies using population-based clinical MRI data remains unexplored. We analyzed clinical MRI data from 23,545 patients in the Capital Region of Denmark. 2,776 patients with mental disorders and 2,066 non-psychiatric controls fulfilled our inclusion and exclusion criteria. Patients with mental disorders exhibited known atrophy patterns in the thalamus (d=-0.303) and amygdala (d=-0.245), with larger ventricles (d=0.277), and thinner insula (d=-0.191), all $p<0.0001$. Analysis across all ROIs revealed widespread cortical thinning (d=-0.207), especially in the middle temporal (d=-0.242) and temporal pole (d=-0.241) regions, and increased cerebrospinal fluid (d=0.268). For volumetric measurements, findings were consistent across different inclusion and exclusion criteria but varied for cortical thickness measurements. Utilizing this currently largest population-based MRI cohort for mental disorders, we demonstrate that clinical MRI scans can detect brain structural differences among patients with mental disorders in real-world clinical settings, aiding in the stratification of patients without mental disorders. Cross-disorder analyses reveal shared neuroanatomical changes, including a general brain atrophy, possibly reflecting accelerated ageing patterns. Integrating large-scale clinical MRI data with electronic health records holds promise for improved patient stratification and tracking of disease progression for future longitudinal cross-disorder studies, bridging real-world MRI data with clinical trajectories for further biological subgrouping.

INTRODUCTION

Prior brain imaging studies aiming to identify brain patterns in mental disorders have often been constrained by small sample sizes with publication bias towards positive findings, highlighting the critical need for larger datasets to ensure reproducibility.[1,2] Nevertheless, Magnetic Resonance Imaging (MRI) scans have proven effective in detecting subtle brain changes across various mental disorders in large-scale studies.[3]

To produce more reliable results, the pioneering consortium ENIGMA (Enhancing NeuroImaging Genetics through Meta-Analysis)[4] pools neuroimaging data from multiple research centers worldwide to increase statistical power and generalize findings across different mental disorders. Despite their studies being the largest to date,[3, 5-10] heterogeneity in imaging protocols, MRI processing, inclusion and exclusion criteria for patients and controls regarding diagnoses, treatments, and demographics across centers might introduce noise and hinder the generalizability of their findings. Additionally, the lack of comprehensive patient history information, in connection to the ENIGMA MRI data, constrains their ability to correlate brain findings with patient clinical data. Most importantly, as the ENIGMA consortia data is the largest dataset to date, validation of their findings in independent large-scale datasets is strongly needed.

Recent advances in automatic tools for extracting cortical and subcortical information from MRI scans have enabled the analysis of clinical MRI data,[11,12] available in quantities far exceeding typical research study samples. Clinical MRI data, often accompanied by electronic health records (EHRs), allows for better patient stratification and more precise inclusion and exclusion criteria based on complete patient histories. Furthermore, as recent advances have shown shared clinical and genetic features across the spectrum of mental disorders,[28,29] cross-disorder investigations are increasingly conducted within psychiatric research.[16-30]

Given these advancements, our study has two primary objectives: First, to assess whether prior findings based on high-quality data can be replicated with routinely acquired clinical MRI scans. Second, to investigate the influence of inclusion and exclusion criteria based on medication and patient history on brain changes associated with mental disorders, both cross-disorder and within diagnostic subgroups. By addressing these objectives, we aim to highlight the potential of large-scale clinical MRI data for advancing the understanding of the neurobiological mechanisms underlying mental disorders and exploring the utility of current real-world MRI in contributing to diagnostic biomarkers.

METHODS

We conducted a retrospective cohort study utilizing all clinical MRI scans from the Capital Region of Denmark acquired during the year 2019, totaling 313,927 MRI images obtained during 28,129 MRI visits on 23,545 unique patients. We first defined our cases with mental disorders and non-psychiatric control using complete EHRs available for all patients, including demographics, diagnoses, and medications. Secondly, anatomical brain regions of interest were defined based on prior large-scale studies and meta-analyses comparing mental disorder patients with controls, to investigate the reproducibility of previous findings. Lastly, we explored the robustness and dynamics of these differences by adding stricter exclusion criteria for cases and non-psychiatric controls. We obtained legal and ethical approvals for the

proposed study from the Data Protection Agency and the Ethics Committee of the Capital Region of Denmark (R-22002033, and P-2020-101).

Study Participants

Individuals ≥18 years of age with mental disorders were included as cases using the following ICD-10 codes: any Mental Disorders (F00-F99), and specifically Dementia (F00-F03 and G30), Substance Use Disorder (F10-19), Schizophrenia Spectrum Disorder (F20-29), Depression (F32-F33), and Anxiety Disorder (F40-F48). For patients with multiple of these diagnoses, a hierarchy was applied—Dementia, Schizophrenia Spectrum Disorder, Depression, Anxiety Disorder, and Substance Use Disorder—based on decreasing ICD-10 code values. Substance Use Disorder was placed last to avoid overriding other psychiatric diagnoses and isolate the effect of substance abuse. Individuals had to be diagnosed with a mental disorder within three months of the MRI scan. This threshold was determined through sensitivity analysis (**Supplementary Figure S1**). Controls were ≥18 years of age and without mental or neurological disorders. These basic inclusion and exclusion criteria were termed "Population A", similar to the minimum criteria to be included in ENIGMA consortium studies. "Population B" additionally included brain medications as exclusion criteria for non-psychiatric controls. Lastly, further exclusions were based on neurological medications and neurological comorbidities for cases ("Population C"). Details for each criteria are provided in **Figure 1**, and specific medication and diagnosis codes are listed in **Supplementary Methods**. Subgroup analyses included only diagnoses with ≥50 individuals meeting Population C criteria, to minimize false-positive findings and overestimation of effect sizes.[1,2] Cross-disorder analyses included all mental disorders (F00–F99, G30) to investigate neuroanatomical patterns shared across the diagnostic spectrum.

MRI Processing

The analysis focused solely on T1-weighted scans due to their superior contrasts for anatomical structures. We estimated T1-weighted sequences from all available MRI scans, resulting in 80,624 T1-weighted scans (**Supplementary Methods**). Each T1-weighted DICOM sequence was converted to NIfTI using dcm2niix.[13] We processed each T1w NIfTI scan with recon-all-clinical[11,12,14,15] to obtain volumetric and cortical thickness estimates. Measurements were averaged bilaterally for regions of interest (ROIs), **Supplementary Figure S2**. Low-quality measurements predicted by recon-all-clinical were automatically discarded.[11] Additional quality control involved removing extreme outliers based on interquartile ranges (below or above 2 for each ROI, **Supplementary Methods**). Our quality control steps and inclusion and exclusion criteria allowed us to detect and remove any potential MRI scans exhibiting significant brain anomalies. For patients with multiple MRI scans passing quality control, inclusion, and exclusion criteria, the best-predicted scan from recon-all-clinical was used. When performing a sensitivity analysis on slice thickness, we first applied the high- and low-resolution threshold before selecting the best-predicted scan per patient, thereby increasing our sample size and overlap between the two groups. All MRI processing steps are illustrated in **Figure 1** and detailed in **Supplementary Methods**.

Outcomes of interest

We aimed to replicate known differences between mental disorder patients and non-psychiatric controls, and dementia patients and non-psychiatric controls, based on ROIs identified in previous studies examining regions affected across disorders (10 ROIs: Lateral Ventricles, Thalamus, Amygdala, Hippocampus, Cortical Thickness, Pars Opercularis Thickness, Medial Orbital Frontal Thickness, Rostral Anterior Cingulate Thickness, Superior Temporal Thickness, and Insula Thickness),[3,5-10,16,17] and well-known studies for dementia (4 ROIs: Lateral Ventricles, Hippocampus, Cortical Thickness, Entorhinal Thickness).[18-20] For mental disorder subgroups, we identified the following ROIs from previous ENIGMA studies: Substance Use Disorder (7 ROIs: Amygdala, Hippocampus, Insula Thickness, Middle Temporal Thickness, Paracentral Thickness, Precentral Thickness, and Supramarginal Thickness),[9] Schizophrenia Spectrum Disorder (12 ROIs: Hippocampus, Amygdala, Thalamus, Nucleus Accumbens, Pallidum, Lateral Ventricles, Cortical Thickness, Fusiform Thickness, Inferior Temporal Thickness, Middle Temporal Thickness, Superior Temporal Thickness, and Insula Thickness),[5,6] Depression (8 ROIs: Hippocampus, Amygdala, Lateral Ventricles, Posterior Cingulate Thickness, Fusiform Thickness, Insula Thickness, Medial Orbitofrontal Thickness, Rostral Anterior Cingulate Thickness),[7,8] and Anxiety Disorder (4 ROIs: Putamen, Pallidum, Hippocampus, and Amygdala).[10]

Statistical Analyses

We reported group differences in brain volumes and cortical thickness between cases with mental disorders and non-psychiatric controls for each ROI with multiple linear regression models using statsmodels.[21] A binary variable, “diagnosis” (0=non-psychiatric controls, 1=patients), was the predictor of interest. We included sex, age, intracranial volume obtained with recon-all-clinical, MRI manufacturer’s model name, and scanner software version (up to major releases) as covariates in the model. To ease comparisons with prior ENIGMA studies,[5-10] effect size estimates were calculated using Cohen’s d[22] computed from the t-statistic of the “diagnosis” variable from the regression models (Equation 10).[23] The 95% confidence intervals were derived using Equation 15,[23] utilizing the asymptotic standard error from Equation 17.[23] For each comparison, we reported uncorrected two-tailed p-values for the t-statistics of the “diagnosis” binary variable from the linear regression model, accompanied by an “*” in case of significance after multiple comparisons correction for each patient group (Bonferroni, $\alpha=0.05$).[24] The number of hypotheses for Bonferroni correction corresponds to the number of ROIs used in each patient group comparison.

RESULTS

In the Capital Region of Denmark, a total of 313,927 MRI images were conducted in 28,129 MRI visits during the year 2019 on 23,545 unique patients. Out of these, a total of 4,842 subjects (2,776 cases and 2,066 non-psychiatric controls) fulfilled the inclusion and exclusion criteria under the most inclusive criteria (Population A), followed by 4,159 subjects for Population B (2,776 cases and 1,383 non-psychiatric controls), and 2,169 subjects for Population C (786 cases and 1,383 non-psychiatric controls) (**Table 1** and **Figure 1**). Most MRI scans were acquired with Philips and Siemens scanners using 3D acquisitions, with magnetic fields of either 1.5T or 3T and slice thicknesses ranging between 1 and 6 mm, with peaks around 1-3 mm. There were no substantial differences in MRI scanner manufacturers, acquisition protocols, or slice thicknesses across criteria (**Supplementary Figure S3**).

MRI differences among individuals with Mental Disorders compared to non-psychiatric controls

Results for Population A, B, and C are presented in **Figure 2A-C**, with numerical values in **Supplementary Table S9**, **Table S10**, and **Table S11**. Under Population C, all comparisons between our clinical MRI data and prior mega-analyses[3,5-10,16,17] were significant, also after correction for multiple comparisons. Mental disorder patients showed smaller volumes in the thalamus (d=-0.303), amygdala (d=-0.245), and hippocampus (d=-0.144), larger lateral ventricular volume (d=0.277), and general cortical thinning (d=-0.207), particularly in the insula (d=-0.191).

For cortical thickness, most comparisons under Population A and B showed no significant differences between mental disorder patients and non-psychiatric controls, with increased cortical thinning in unmedicated patients and those without brain comorbidities (Population C d=-0.207 vs. Population B d=-0.078). Consistent findings were observed across criteria for volumetric measures, despite Population C having approximately 3.5 times fewer cases and 1.5 times fewer non-psychiatric controls than Population A.

Dementia patients exhibited large effect sizes: smaller hippocampal volume (d=-0.651), larger lateral ventricles (d=0.761), and general cortical thinning (d=-0.663), especially in the entorhinal cortex (d=-0.747). To ensure that our findings for mental disorders were not biased by large effect sizes in the dementia subgroup, we performed analysis excluding dementia patients and reassessed Population C (**Figure 2C**). Effect sizes were smaller but consistent with previous findings and all comparisons, except for the hippocampus, were still significant after correction for multiple comparisons.

We identified additional brain differences not reported as main findings in prior ENIGMA studies[3,5-10,16,17] under Population C (**Figure 3**). After correcting for multiple comparisons across all ROIs, we identified 38 significant differences, highlighting a general thinning pattern across most cortical areas (cortical thickness d=-0.207, middle temporal d=-0.242, temporal pole d=-0.241, and superior frontal d=-0.229), smaller deep gray matter structures (thalamus d=-0.303, amygdala d=-0.245, nucleus accumbens d=-0.179 and pallidum d=-0.175), and larger ventricular volumes (inferior lateral ventricles d=0.363, 3rd ventricle d=0.320 and lateral ventricles d=0.277). We also reported higher amounts of extracerebral CSF (d=0.268). These differences were also found for Population A (**Supplementary Figure S4**) and B (**Supplementary Figure S5**), although to a smaller extent, especially regarding cortical thinning (19 and 27 significant differences, respectively).

Comparison between mental disorder subgroups and non-psychiatric controls

For Population B, statistically significant brain differences between mental disorder subgroups and controls were found for 20 of 32 ROIs; and after correction for multiple comparisons, 16 of 32 remained significant (**Figure 4**). Population A and C yielded 13 and 10 significant comparisons, respectively (**Supplementary Figure S6** and **Supplementary Figure S7**). Effect sizes were generally consistent but smaller compared to ENIGMA studies, and most non-significant differences are related to subcortical thickness areas. For the Substance Use Disorder subgroup, we observed larger effect sizes for the amygdala, hippocampus, and insula than previously reported.[9] Schizophrenia Spectrum Disorder subgroup comparisons revealed consistent cortical thinning and atrophy in deep gray matter

structures with ENIGMA studies,[5,6] with only opposite findings for the hippocampus, lateral ventricles, and pallidum. For the Depression subgroup, effect sizes were similar for most comparisons, although not significant, while we noticed a large effect for lateral ventricles compared to ENIGMA.[7,8] For Anxiety Disorders, we only reported a negative effect for the pallidum in contrast with ENIGMA.[10]

Effect of Slice Thickness

We assessed the influence of MRI slice thickness on our findings by separating scans into high-resolution (<1.5 mm) and low-resolution (≥1.5 mm) groups (approximately 40% of cases and non-psychiatric controls overlapped between high- and low-resolution groups). Results for Population C are shown in **Figure 2D**. Volumetric comparisons were consistent, while slight differences were observed for cortical thickness comparisons. Similar results were found across criteria for volumetric comparisons, with larger differences in cortical thickness comparisons (**Supplementary Figure S8**).

DISCUSSION

To our knowledge, this is the first large-scale population-based neuroimaging study using real-world clinical MRI scans to investigate brain changes in mental disorders. We successfully replicated many previously reported findings from meta-analyses of brain differences between patients with mental disorders and non-psychiatric controls, as well as between patients with dementia and non-psychiatric controls. However, when examining mental disorder subgroups, we observed smaller effect sizes than those reported in previous meta-analyses. This discrepancy likely stems from differences in the definition of our control group, which included patients undergoing MRI scans for possible brain-related conditions, highlighting future avenues for predicting changes in a more challenging control cohort than typically used in research studies relying on healthy controls. This study is also the largest to date that investigates brain changes associated with mental disorders as a whole, rather than focusing on specific subgroups, as seen in previous ENIGMA studies.[3] Our findings reveal a general atrophy pattern across cortical areas and deep gray matter structures among patients with mental disorders, reflecting possible accelerated brain ageing,[31,32] and suggesting that clinical MRI data, supplemented with EHR information, can identify biomarkers for mental disorders and improve patient diagnosis and trajectories.

Our exclusion criteria, based on brain medications and comorbidities from EHRs, influenced our findings. We noted consistent effect sizes for volumetric measurements when applying stricter exclusion criteria, even though our sample sizes decreased 1.5-fold for cases and 3.5-fold for non-psychiatric controls. We also observed increased cortical thinning in unmedicated patients and those without brain comorbidities compared to the overall patient group, leading to contrasting findings when applying different exclusion and inclusion criteria. Additionally, we found that effect sizes for the Substance Use disorders group were substantially larger for Population C than those reported in a previous ENIGMA study,[9] as well as our Population A and B, suggesting that different inclusion and exclusion criteria might play an even bigger role, thus warranting further investigation.

When examining mental disorder subgroups, the effect sizes were generally in the same direction as in the ENIGMA studies but often not significant after correcting for multiple

comparisons. This might be due to the larger sample sizes in the combined ENIGMA studies, which translate into more significant comparisons, even with small effect sizes. Additionally, our findings suggest that cortical thickness changes are more challenging to detect in clinical MRI scans due to the subtlety of these changes and the lower resolution and quality of clinical images. However, comparing the effect sizes in our study with those reported in ENIGMA studies is complex. Discrepancies in inclusion and exclusion criteria, processing tools, and MRI scan quality between the ENIGMA and our studies likely impact the findings. We used Population B to closely match those in ENIGMA studies. However, several centers in prior ENIGMA studies employed less strict protocols, especially for cases, that are more similar to our less strict criteria (Population A). Indeed, under our strictest criteria (Population C), we observed the least significant comparisons with ENIGMA studies.

The main strength of this study is the use of a large-scale population-based MRI dataset from real-world clinical settings. The integration of EHRs allows for rigorous and flexible inclusion and exclusion criteria, enabling a better understanding of the impact of medication and comorbidities on brain structure, a better match with prior studies' inclusion and exclusion criteria, and enhancing the ability to track disease progression and correlate brain changes with patient histories.

Limitations include our real-world data with clinical MRI scans being typically of lower quality than those used in research studies. Our findings suggest that differences in effect sizes are only to a small degree influenced by the slice thickness of the scans, particularly for cortical thickness measurements. Furthermore, we could not use established automatic methods like FreeSurfer,[25] FSL,[26] and SPM,[27] as these tools cannot yet handle the low-resolution MRI scans in our clinical cohort. Instead, we employed recently developed automatic tools[10,11] to obtain cortical and subcortical measurements, which might require further validation.

Our cohort is the largest population-based cohort, yet smaller than the combined worldwide cohorts in prior ENIGMA mega-analyses studies. However, our study is based on MRI scans acquired in a single year (2019) only, thus, there is substantial potential in future studies to mitigate the subtle nature of subcortical differences, where more data is needed to validate our findings further. Moreover, we did not age- and sex-match controls in this study due to the limited sample size, but we adjusted for these covariates in our analysis. Our sample size was also yet insufficient for studying brain changes in other mental disorders such as bipolar disorder, attention-deficit/hyperactivity disorder, and autism spectrum disorder.

Clinical MRI scans can effectively detect cortical and subcortical differences among patients with mental disorders and also distinguish them from other patients without mental disorders. When examining mental disorder subgroups, we observed consistent, though smaller, effect sizes compared to previous ENIGMA mega-analyses studies using high-quality MRI data. These differences are likely due to our control group comprising patients undergoing MRI scans for potential clinical diagnoses. In contrast, the studies in the ENIGMA mega-analyses compare to healthy controls, which makes prediction easier, whereas, in a real-world clinical context, the separation from other individuals undergoing examination is of importance for specificity. The integration of EHR data allows for the application of stricter inclusion and exclusion criteria, enabling more accurate analysis of correlations between medication, brain comorbidities, and brain changes.

Our findings reveal brain differences across mental disorders consistent with accelerated aging. Factors such as slice thickness, comorbidities, and medication can affect the detection of structural changes. Population selection should reflect the study objective: real-world clinical samples (Population A) capture brain patterns representative of routine care but introduce greater heterogeneity, whereas strictly defined samples (Population C) minimize variability and improve specificity, at the cost of broader generalizability. We recommend standardizing inclusion/exclusion criteria, incorporating EHR-based comorbidity data, and leveraging routine clinical MRI scans—including lower-resolution images—to enable large-scale biomarker discovery while accounting for scan quality. These strategies can support more precise investigations of neurobiological mechanisms and advance diagnostic and therapeutic approaches.

ACKNOWLEDGEMENTS

Stefano Cerri has received funding from the Lundbeck Foundation (R449-2023-1512). Mostafa Mehdipour Ghazi has received funding from the Lundbeck Foundation (R400-2022-617). Mads Nielsen is supported by the Pioneer Centre for AI, Danish National Research Foundation, grant number P1. Michael Eriksen Benros has received funding from the Lundbeck Foundation (R278-2018-1411 and R383-2022-285).

References:

1. Ioannidis, J. P. (2011). Excess significance bias in the literature on brain volume abnormalities. Archives of general psychiatry, 68(8):773–780.

2. Button, K. S., Ioannidis, J. P., Mokrysz, C., et al. (2013). Power failure: why small sample size undermines the reliability of neuroscience. Nature reviews neuroscience, 14(5):365–376.

3. Thompson, P. M., Jahanshad, N., Ching, C. R., et al. (2020). ENIGMA and global neuroscience: A decade of large-scale studies of the brain in health and disease across more than 40 countries. Translational psychiatry, 10(1):100.

4. Thompson, P. M., Stein, J. L., Medland, S. E., et al. (2014). The ENIGMA Consortium: large-scale collaborative analyses of neuroimaging and genetic data. Brain imaging and behavior, 8:153–182.

5. Van Erp, T. G., Hibar, D. P., Rasmussen, J. M., et al. (2016). Subcortical brain volume abnormalities in 2028 individuals with schizophrenia and 2540 healthy controls via the ENIGMA consortium. Molecular psychiatry, 21(4):547–553.

6. Van Erp, T. G., Walton, E., Hibar, D. P., et al. (2018). Cortical brain abnormalities in 4474 individuals with schizophrenia and 5098 control subjects via the enhancing neuro imaging genetics through meta analysis (ENIGMA) consortium. Biological psychiatry, 84(9):644–654.

7. Schmaal, L., Veltman, D. J., van Erp, T. G., et al. (2016). Subcortical brain alterations in major depressive disorder: findings from the ENIGMA Major Depressive Disorder working group. Molecular psychiatry, 21(6):806–812.

8. Schmaal, L., Hibar, D., S¨amann, P. G., et al. (2017). Cortical abnormalities in adults and adolescents with major depression based on brain scans from 20 cohorts worldwide in the ENIGMA Major Depressive Disorder Working Group. Molecular psychiatry, 22(6):900– 909.

9. Mackey, S., Allgaier, N., Chaarani, B., et al. (2019). Mega-analysis of gray matter volume in substance dependence: general and substance-specific regional effects. American Journal of Psychiatry, 176(2):119–128.

10. Groenewold, N. A., Bas-Hoogendam, J. M., Amod, A. R., et al. (2023). Volume of subcortical brain regions in social anxiety disorder: mega-analytic results from 37 samples in the ENIGMA-Anxiety Working Group. Molecular psychiatry, 28(3):1079–1089.

11. Billot, B., Magdamo, C., Cheng, Y., Arnold, S. E., Das, S., and Iglesias, J. E. (2023). Robust machine learning segmentation for large-scale analysis of heterogeneous clinical brain MRI datasets. Proceedings of the National Academy of Sciences, 120(9):e2216399120.

12. Gopinath, K., Greve, D. N., Das, S., Arnold, S., Magdamo, C., and Iglesias, J. E. (2023). Cortical analysis of heterogeneous clinical brain MRI scans for large-scale neuroimaging studies. In International Conference on Medical Image Computing and Computer-Assisted Intervention, pages 35–45. Springer.

13. Li, X., Morgan, P. S., Ashburner, J., Smith, J., and Rorden, C. (2016). The first step for neuroimaging data analysis: DICOM to NIfTI conversion. Journal of neuroscience methods, 264:47–56.

14. Billot, B., Greve, D. N., Puonti, O., et al. (2023). SynthSeg: Segmentation of brain MRI scans of any contrast and resolution without retraining. Medical image analysis, 86:102789.

15. Iglesias, J. E., Billot, B., Balbastre, Y., et al. (2023). SynthSR: A public AI tool to turn heterogeneous clinical brain scans into high-resolution T1-weighted images for 3D morphometry. Science advances, 9(5):eadd3607.

16. Hettwer, M., Larivière, S., Park, B., et al. (2022). Coordinated cortical thickness alterations across six neurodevelopmental and psychiatric disorders. Nature communications, 13(1):6851.

17. Goodkind, M., Eickhoff, S. B., Oathes, D. J., et al. (2015). Identification of a common neurobiological substrate for mental illness. JAMA psychiatry, 72(4):305–315.

18. Killiany, R. J., Gomez-Isla, T., Moss, M., et al. (2000). Use of structural magnetic resonance imaging to predict who will get Alzheimer's disease. Annals of Neurology: Official Journal of the American Neurological Association and the Child Neurology Society, 47(4):430–439.

19. Dickerson, B. C., Goncharova, I., Sullivan, M., et al. (2001). MRI-derived entorhinal and hippocampal atrophy in incipient and very mild Alzheimer's disease. Neurobiology of aging, 22(5):747–754.

20. Apostolova, L. G., Green, A. E., Babakchanian, S., et al. (2012). Hippocampal atrophy and ventricular enlargement in normal aging, mild cognitive impairment (MCI), and Alzheimer Disease. Alzheimer Disease & Associated Disorders, 26(1):17–27.

21. Seabold, S. and Perktold, J. (2010). Statsmodels: econometric and statistical modeling with python. SciPy, 7:1.

22. Cohen, J. (1992). Quantitative methods in psychology: A power primer. Psychol. Bull., 112:1155–1159.

23. Nakagawa, S. and Cuthill, I. C. (2007). Effect size, confidence interval and statistical significance: a practical guide for biologists. Biological reviews, 82(4):591–605.

24. Bonferroni, C. (1936). Teoria statistica delle classi e calcolo delle probabilita. Pubblicazioni del R Istituto Superiore di Scienze Economiche e Commericiali di Firenze, 8:3–62.

25. Fischl, B. (2012). FreeSurfer. Neuroimage, 62(2):774–781.

26. Jenkinson, M., Beckmann, C. F., Behrens, T. E., Woolrich, M. W., and Smith, S. M. (2012). FSL. Neuroimage, 62(2):782–790.

27. Ashburner, J. and Friston, K. J. (2005). Unified segmentation. Neuroimage, 26(3):839–851.

28. Cai N, Verhulst B, Andreassen OA, et al. (2025). Assessment and ascertainment in psychiatric molecular genetics: challenges and opportunities for cross-disorder research. Mol Psychiatry Apr;30(4):1627-1638.

29. Schork AJ, Won H, Appadurai V, et al. (2019). A genome-wide association study of shared risk across psychiatric disorders implicates gene regulation during fetal neurodevelopment. Nat Neurosci. 22(3):353-361.

30. Opel N, Goltermann J, Hermesdorf M, et al. (2020). Cross-Disorder Analysis of Brain Structural Abnormalities in Six Major Psychiatric Disorders: A Secondary Analysis of Mega- and Meta-analytical Findings From the ENIGMA Consortium. Biol Psychiatry.

31. Koutsouleris, N., Davatzikos, C., Borgwardt, S., et al. (2014). Accelerated brain aging in schizophrenia and beyond: a neuroanatomical marker of psychiatric disorders. Schizophrenia bulletin, 40(5), 1140-1153.

32. Han, L. K. M., Dinga, R., Hahn, T., et al. (2021). Brain aging in major depressive disorder: results from the ENIGMA major depressive disorder working group. Molecular psychiatry, 26(9), 5124–5139.

Figure legend

Figure 1: Illustration of the MRI processing pipeline, selected inclusion and exclusion criteria, and analysis. More details are provided in Supplementary Methods.

Figure 2: Comparisons between mental disorders and non-psychiatric controls. Panel A: Patients with mental disorders vs. non-psychiatric controls across inclusion and exclusion criteria. Panel B: Patients with dementia vs. non-psychiatric controls across inclusion and exclusion criteria. Panel C: Patients with mental disorders vs. non-psychiatric controls, excluding dementia patients from the cases group across inclusion and exclusion criteria. Panel D: Impact of slice thickness on differences between patients with mental disorders and non-psychiatric controls for Population C. Results for Population A and B can be found in Supplementary Figure S8. Numerical values for all the figures can be found in Supplementary Table S9 to Table S14.

Figure 3: Mental Disorders vs. non-psychiatric controls. Comparisons for all ROI for Population C. Results for Population A and B can be found in Supplementary Figure S4 and Figure S5. Numerical values for all the figures can be found in Supplementary Table S15 to Table S17.

Figure 4: Mental Disorders Subgroups vs. non-psychiatric Controls. Comparisons with ENIGMA studies for Population B. R: Right, L: Left, and B: Bilateral. Results for Population A and C can be found in Supplementary Figure S6 and Supplementary Figure S7. Numerical values for all the figures can be found in Supplementary Table S18 to Table S20.

Table 1: Demographic of the clinical MRI dataset of individuals with mental disorders and non-psychiatric controls.

	Population A			Population B			Population C		
Group	**N**	**Sex [male/female] [female %]**	**Age [mean ± std] [min, max]**	**N**	**Sex [male/female] [female %]**	**Age [mean ± std] [min, max]**	**N**	**Sex [male/female] [female %]**	**Age [mean ± std] [min, max]**
Mental Disorders (any)	2776	[1590/1186] [43%]	[52.63±18.46] [18, 95]	2776	[1590/1186] [43%]	[52.63±18.46] [18, 95]	786	[459/327] [42%]	[45.52±18.26] [18, 92]
Mental Disorders without Dementia	2608	[1510/1098] [42%]	[51.25±18.02] [18, 95]	2608	[1510/1098] [42%]	[51.25±18.02] [18, 95]	752	[439/313] [42%]	[44.26±17.55] [18, 89]
Dementia	262	[138/124] [47%]	[75.09±9.82] [34, 93]	262	[138/124] [47%]	[75.09±9.82] [34, 93]	60	[35/25] [42%]	[74.18±9.09] [46, 92]
Substance Use Disorder	574	[254/320] [56%]	[58.58±15.06] [19, 90]	574	[254/320] [56%]	[58.58±15.06] [19, 90]	119	[46/73] [61%]	[53.77±14.75] [19, 78]
Schizophrenia Spectrum Disorder	436	[214/222] [51%]	[41.24±17.54] [18, 88]	436	[214/222] [51%]	[41.24±17.54] [18, 88]	215	[103/112] [52%]	[36.20±15.98] [18, 78]
Depression	676	[459/217] [32%]	[53.28±17.00] [18, 91]	676	[459/217] [32%]	[53.28±17.00] [18, 91]	179	[127/52] [29%]	[48.44±16.57] [18, 85]
Anxiety Disorder	524	[254/320] [30%]	[58.58±15.06] [19, 90]	524	[254/320] [30%]	[58.58±15.06] [19, 90]	155	[117/38] [25%]	[43.17±14.88] [18, 84]
Non-Psychiatric Controls	2066	[1220/846] [41%]	[51.37±17.74] [18, 98]	1383	[797/586] [42%]	[48.14±16.95] [18, 98]	1383	[797/586] [42%]	[48.14±16.95] [18, 98]

Population A: Non-Psychiatric Controls: age ≥18, No Mental Disorders, No Neurological Disorder. Cases: age ≥18, Mental Disorders.
Population B: Non-Psychiatric Controls: Population A + No Brain Medications. Cases: Same as Population A.
Population C: Non-Psychiatric Controls: Same as Population B. Cases: Population A + No Neurological Medications, No Neurological Comorbidities.

Figure 1: Illustration of the MRI processing pipeline, with selected inclusion and exclusion criteria, and analysis.

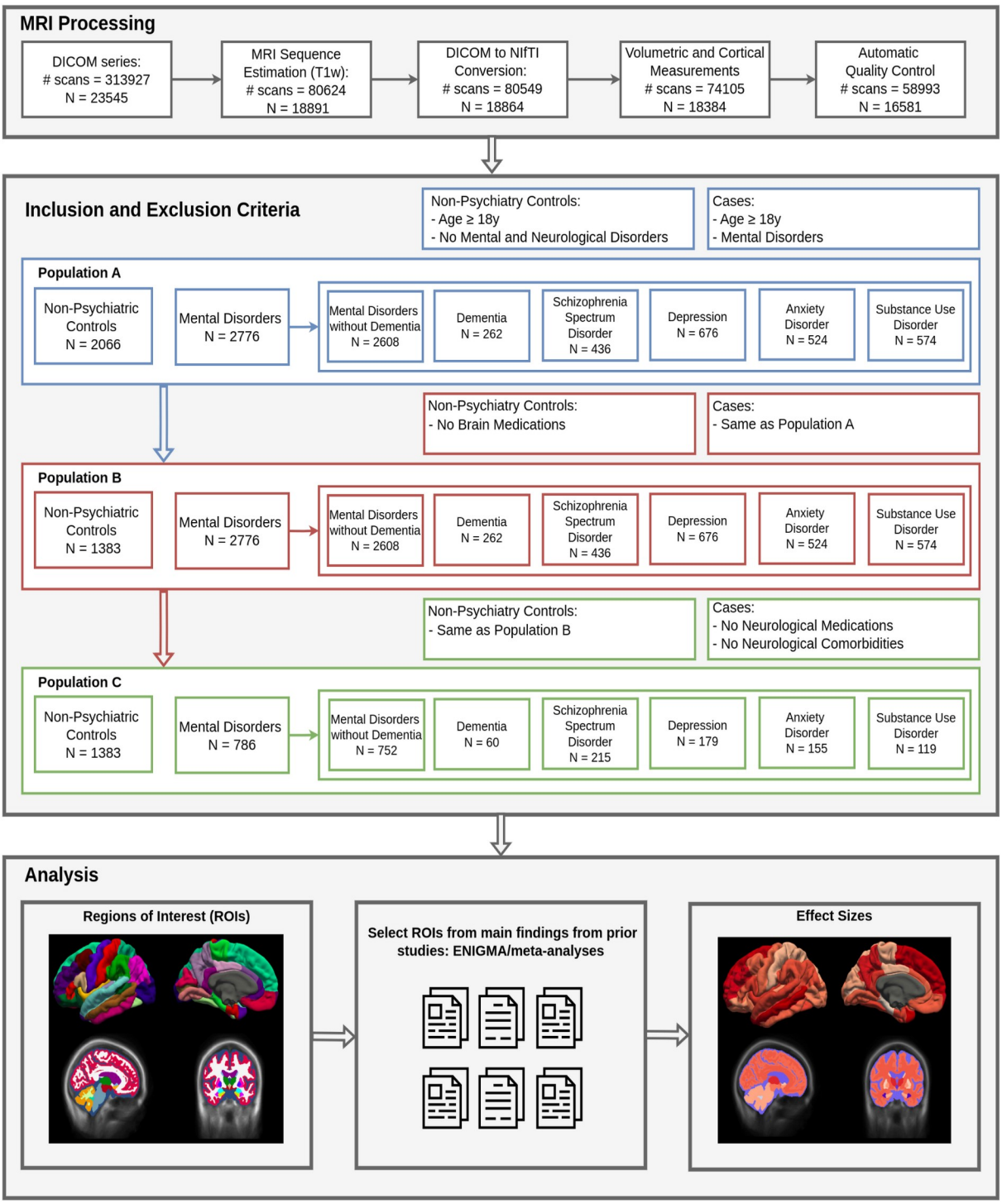

Figure 2: Mental disorders vs. non-psychiatric controls comparisons.

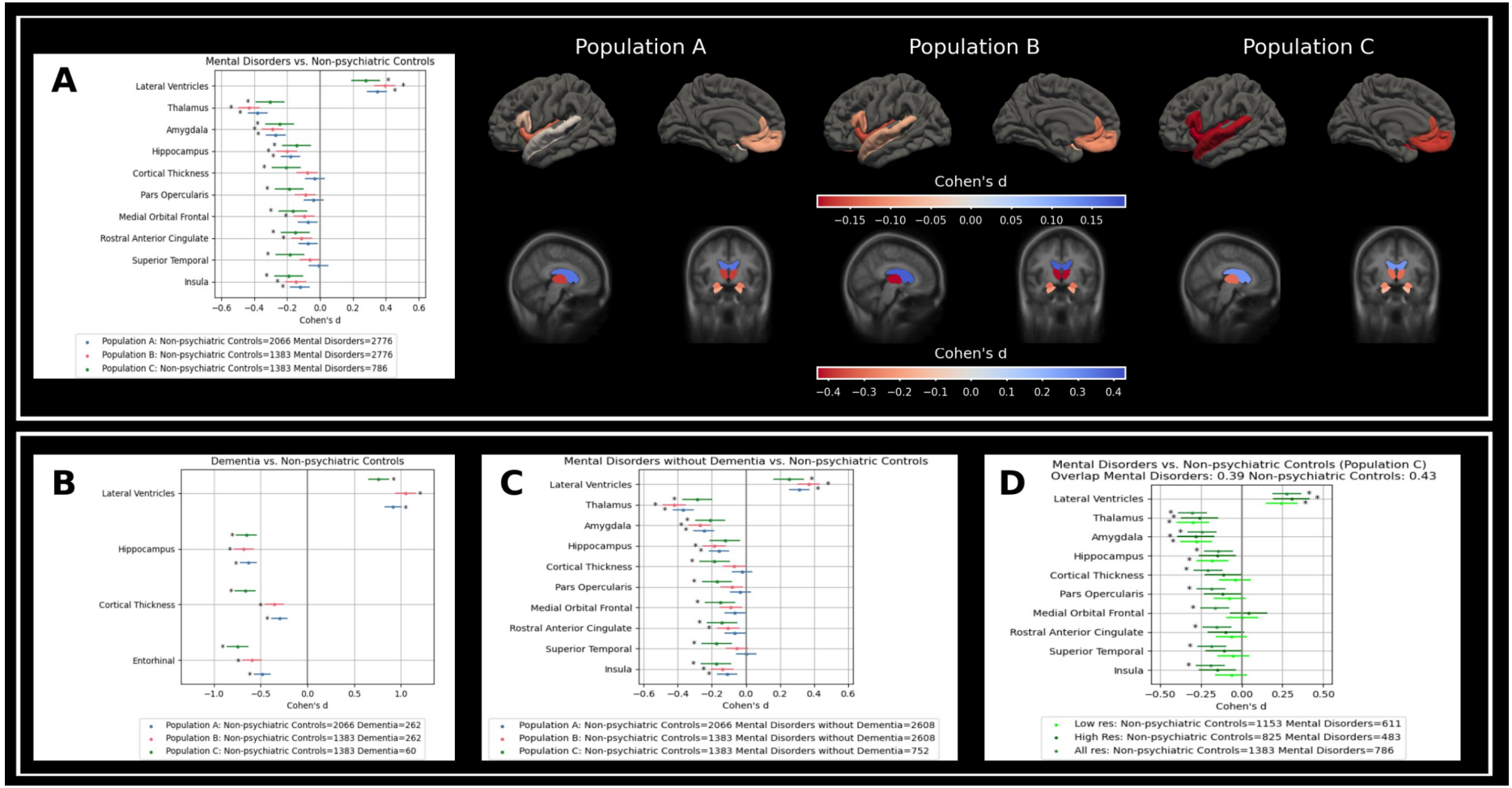

Figure 3: Mental Disorders vs. non-psychiatric controls. Comparisons for all ROI for Population C.

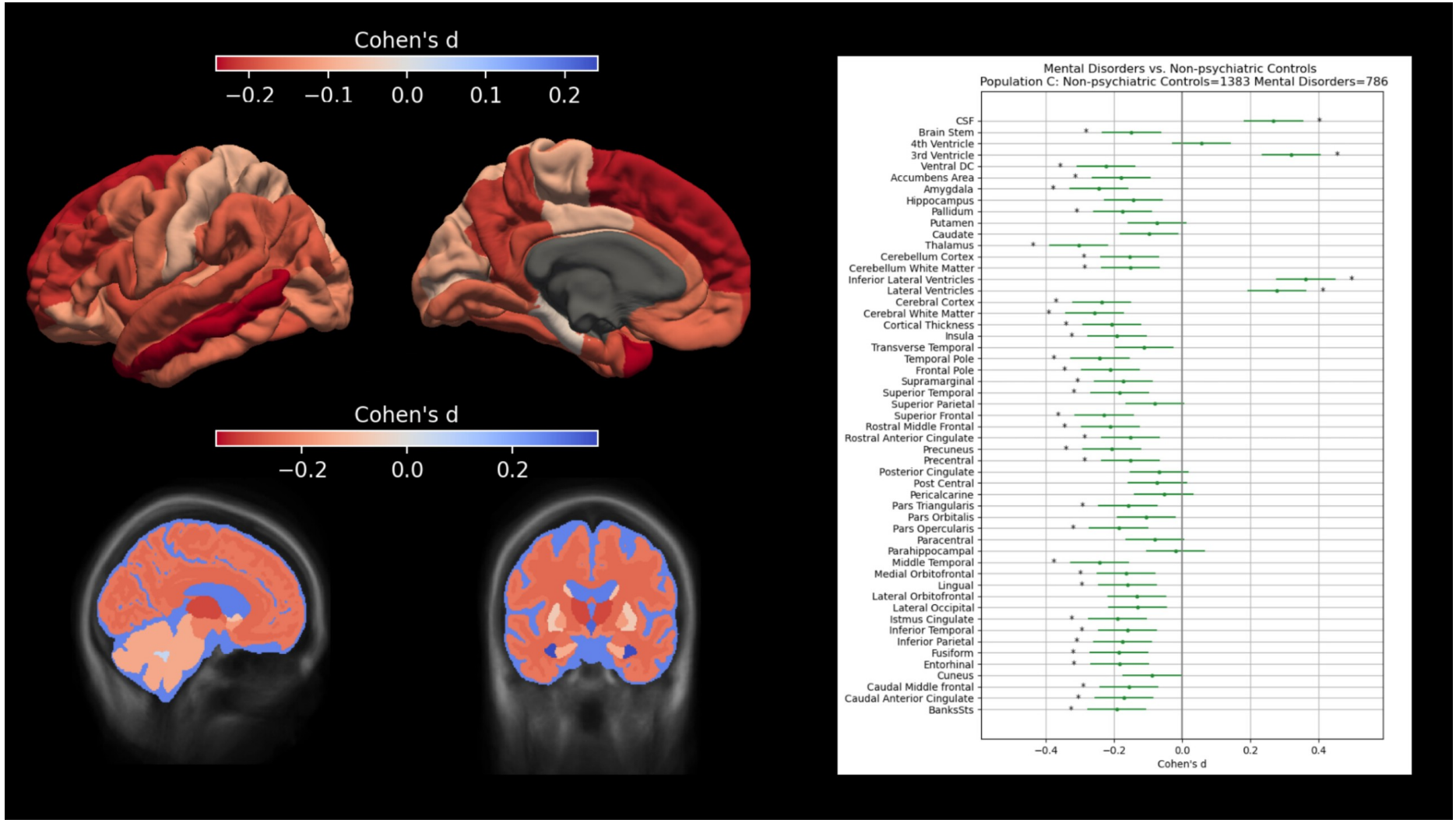

Figure 4: Mental Disorders Subgroups vs. non-psychiatric Controls. Comparisons with ENIGMA studies for Population B.

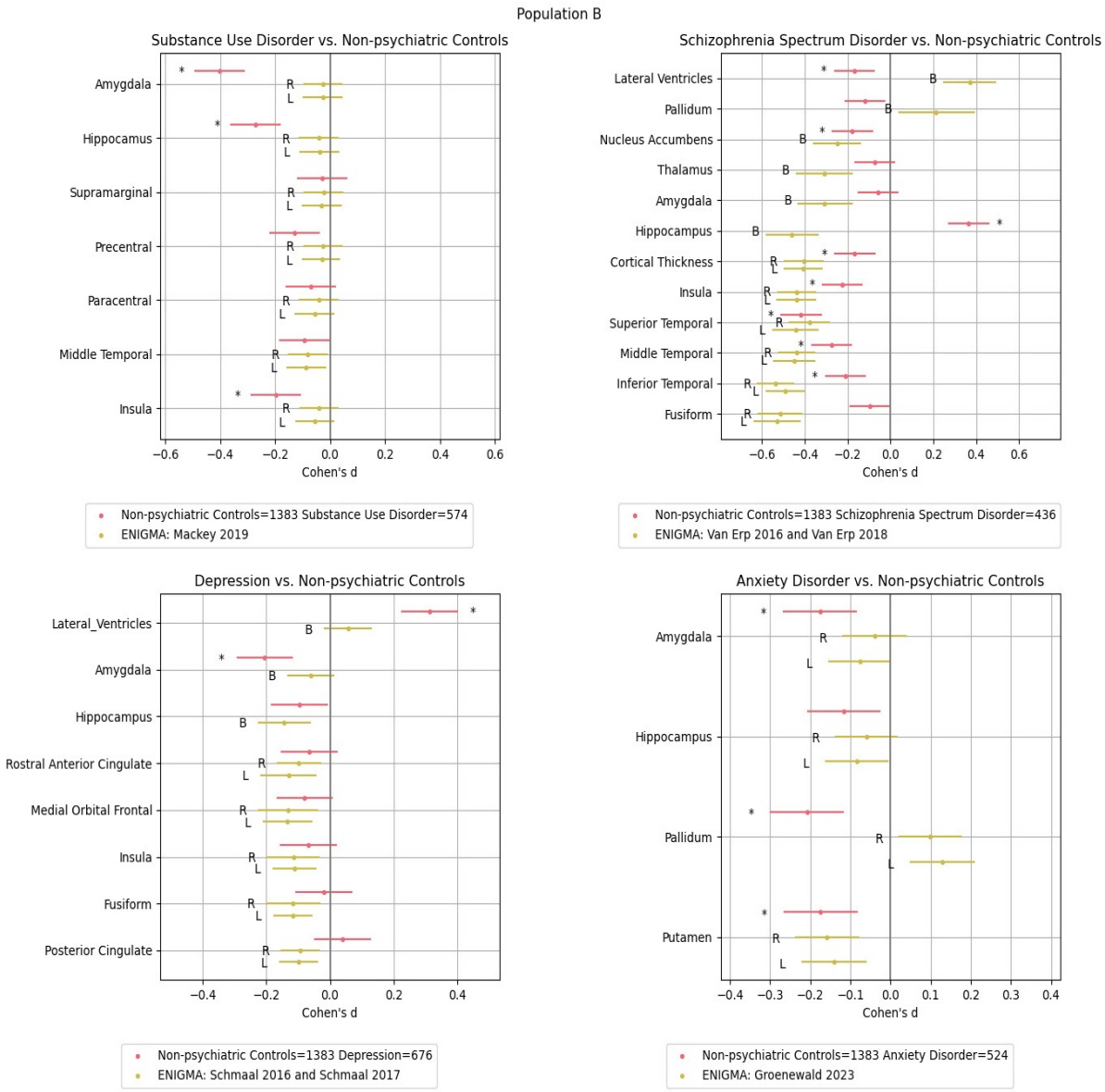

Supplementary Material

Supplementary Methods. MRI processing pipeline, inclusion, and exclusion criteria.
Supplementary Figure S1. Sensitivity analysis on the number of unique patients who received a diagnosis either before or after the MRI scan was taken, measured in months, and included patients who were diagnosed within 3 months before or after the date of the MRI.
Supplementary Figure S2. Regions of interest.
Supplementary Figure S3. MRI dataset information.
Supplementary Figure S4. Comparisons of all ROIs for Population A.
Supplementary Figure S5. Comparisons of all ROIs for Population B.
Supplementary Figure S6. Comparison of findings between mental disorders subgroups and controls, with prior ENIGMA studies for Population A.
Supplementary Figure S7. Comparison of findings between mental disorders subgroups and controls, with prior ENIGMA studies for Population C.
Supplementary Figure S8. Comparison of findings for high- (<1.5mm slice thickness) and low-resolution (>1.5mm slice thickness) scans for Population A and Population B.
Supplementary Table S9. Comparison of mental disorders and dementia patients for previously reported ROI differences for Population A.
Supplementary Table S10. Comparison of mental disorders and dementia patients for previously reported ROI differences for Population B.
Supplementary Table S11. Comparison of mental disorders and dementia patients for previously reported ROI differences for Population C.
Supplementary Table S12. Comparison of findings for high- (<1.5mm slice thickness) and low-resolution (≥1.5mm slice thickness) scans for Population A.
Supplementary Table S13. Comparison of findings for high- (<1.5mm slice thickness) and low-resolution (≥1.5mm slice thickness) scans for Population B.
Supplementary Table S14. Comparison of findings for high- (<1.5mm slice thickness) and low-resolution (≥1.5mm slice thickness) scans for Population C.
Supplementary Table S15. Comparisons of all ROIs for Population A.
Supplementary Table S16. Comparisons of all ROIs for Population B.
Supplementary Table S17. Comparisons of all ROIs for Population C.
Supplementary Table S18. Comparison of findings between mental disorders subgroups and controls, with prior ENIGMA studies for Population A.
Supplementary Table S19. Comparison of findings between mental disorders subgroups and controls, with prior ENIGMA studies for Population B.
Supplementary Table S20. Comparison of findings between mental disorders subgroups and controls, with prior ENIGMA studies for Population C.

Supplementary Methods: MRI processing pipeline, inclusion, and exclusion criteria

This section describes how we processed the clinical MRI dataset and selected the inclusion and exclusion criteria.

1) MRI sequence estimation

We assigned every scan to one or multiple of the following categories: Fluid-attenuated inversion recovery (FLAIR), Diffusion- (DWI), Susceptibility- (SWI), T1- (T1), T2-weighted imaging (T2* excluded), as well as other identified sequences. The categorization was performed by checking the DICOM header entry Series Description (0008,103E) for the following substrings:

- T1-weighted imaging: ‘T1’, ‘t1’, ‘BRAVO’, ‘mprage’, ‘MPRAGE’ (49,108 scans);
- T2-weighted imaging: ‘T2’, ‘t2’ (47,679 scans);
- Fluid-attenuated inversion recovery: ‘FLAIR’, ‘flair’, ‘Flair’ (21,322 scans);
- Susceptibility-weighted imaging: ‘SWI’, ‘swi’, ‘SUSCEPTABILITET’ (20,434 scans);
- Diffusion-weighted Imaging: ‘DWI’, ‘dwi’, ‘MUSE’, ‘Diffusion’, ‘DTI’, ‘dti’, (35,521 scans);
- Other identified sequence types: ’vessel scout’, ‘VRT’, ‘csf flow’, ‘WIP’, ‘svs’, ‘SVS’, ‘animation’, ‘ACOM’, ‘Verification’, ‘BA’, ‘BLACK BLOOD’, ‘Batch’, ‘Cerebral Blood Flow’, ‘DISPLAY’, ‘IMPAX Volume’, ‘MYELO’, ‘MI Reading’, ‘MM Oncology Reading’, ‘SCREENSAVE’, ‘SPINE’, ‘3D Saved State - AutoSave’, ‘Screen Save’, ‘MINIP’, ‘Minimum Intensity’, ‘Min Intensity Projection’, ‘Min Intensity ’, ‘Minimum Intensity Projection’, ‘Tra SWIp MinIP’, ‘BOLD’, ‘Loc’, ‘loc’, ‘Scout’, ‘LOC’, ‘lokal’, ‘LOKAL’, ‘B1 Calibration’, ‘calib’, ‘Calib’, ‘cal’, ‘Cal’, ‘CAL’, ‘PDW’, ‘TOF’, ‘ToF’, ‘tof’, ‘angio’, ‘Angio’, ‘ANGIO’, ‘SWAN’, ‘PCA’, ‘pca’, ‘dce’, ‘PC’, ‘pc’, ‘TRANCE’, ‘trance’, ‘mIP’, ‘MIP’, ‘SURVEY’, ‘Survey’, ‘survey’, ‘CEST’, ‘ASL’, ‘asl’, ‘TRACEW’, ‘travew’, ‘STIR’, ‘stir’, ‘ADC’, ‘Apparent Diffusion Coefficient’, ‘adc’, ‘Perfusion Weighted’, ‘T2*’, ‘t2*’ (71,814 scans).

Based on the categorization, the second step was constructing classes used as training and prediction targets. Scans from the T2 category are assigned to the T2 class except those in the FLAIR category, which were then assigned to the FLAIR class. The intersection of FLAIR and T2 categories occurs because FLAIR is a T2-weighted MRI technique modification often called “T2-FLAIR”. Scans in other intersections of categories were assigned to the “Unlabeled” class. We predicted a label (FLAIR, DWI, SWI, T1, T2, or other identified sequence) for every unlabeled scan (N=71,049), after training and validation on the labeled data (N=242,878). As input features, we used non-private DICOM header tags that might be related to the sequence type. Tags with more than half the entries missing are discarded. The remaining tags used for classification are:

- (0018,0081) Echo Time;
- (0018,0080) Repetition Time;
- (0018,1314) Flip Angle;
- (0018,0091) Echo Train Length;
- (0018,0020) Scanning Sequence;
- (0018,0021) Sequence Variant;
- (0018,1318) dBdt;
- (0018,0021) Scan Options;
- (0018,0084) Imaging Frequency;
- (0018,0086) Echo Numbers.

Missing numeric values were replaced by the median of the feature computed over all scans. The scanning sequence (SS), sequence variant (SV) and, scan options (SO), image type (IT) features were one-hot encoded, i.e., every distinct possible entry (e.g., Spin Echo, Inversion Recovery, Magnetization Transfer Contrast, etc) is represented by a binary vector. Entries that occurred in less than 1% of all training samples were dropped. Some entries occurred under multiple tags, e.g., Inversion Recovery was present under the Scan Options and the Scanning Sequence tag. These were combined with an OR statement to one binary feature. For SV, SS, and SO

tags, empty lists were also converted to binary features. The preprocessing results in 74 features (67 binary, 6 continuous, and 1 discrete). Labeled data is split into a train (N=218,590) and a validation set (N=24,288). XGBoost (xgboost, v.2.0.3)[1] was used for classification. To find good hyperparameters, 5-fold cross-validation was performed using Bayesian optimization. For more robust classification performances, tuning and training of the classifier were repeated 5 times with different initializations of the model's parameter, and majority voting was performed to obtain the final classification. In the case of ties, the T1w class was picked. After sequence prediction, we obtained 80,624 T1w, 51,685 T2w, 24,290 FLAIR, 23,406 SWI, 34,383 DWI, and 99,539 "other" scans.

2) MRI Dicom to NIfTI conversion

We converted to NIfTI all the 80,624 T1w DICOM series obtained after the MRI sequence estimation with dcm2niix (v.1.0.20230411)[2]. 75 conversions resulted in an error and the corresponding scans were discarded. When multiple NIfTI scans were obtained from a single DICOM series, the largest converted file was kept for further processing.

3) Recon-all-clinical

We processed each of the 80,549 converted NIfTI T1w scans with recon-all-clinical[3-6] (FreeSurfer v. 7.4.1). 6,444 scans resulted in errors; this is due to a limited field of view of the images, 2D images, or MRI pathologies that result in an error at any step of the pipeline.

4) Automatic Quality Control

Recon-all-clinical provides estimated Dice[7] scores for the following brain structures:[5] white matter, cortex, lateral ventricle, cerebellum, thalamus, hippocampus, amygdala, pallidum, putamen, and brainstem. We considered a segmentation failure when the Dice score of any structure listed above was below 0.65[5]. 11,549 scans were discarded.

All regions of interest (ROIs) of Sections 3.2 and 3.3, normalized for intracranial volume, with a volume or thickness larger or smaller than 2 times the interquartile range were discarded for further automatic quality control. 3,563 scans were discarded. 58,993 scans remained after automatic quality control.

5) Inclusion and exclusion criteria

We have the following three populations based on different criteria for inclusion and exclusion. Diagnostic and medication codes were based on ICD-10 Version: 2019[8]:

Population A:

Non-psychiatric Controls:

For non-psychiatric controls, the following criteria were used:

- No psychiatric diagnosis (F00-F99, G30) before or within 3 months after the acquisition of the MRI scan;
- age >= 18 years at the time of the MRI scan;
- No neurological comorbidities:
    - Nervous system: G00-DG99, except G560 (Carpal tunnel syndrome) and G562 (Ulnar nerve neuropathy);
    - Cerebrovascular diagnosis: I60-69, E236E;
    - CNS infections: A022C, A066, A17, A229C, A321, A390, A504, A514B, A521A–B, A548A, A80–A89, B003–B004, B010–B011, B020–B021, B050–B051, B060, B261–B262, B375, B451, B582, B602, E236A;
    - Traumatic brain injury: S060-S069;

- Skull fracture: S020, S021, S027, S029;
- Malignant cancer: C00-C99;
- Benign neoplasm in the nervous system: D32-D33;
- HIV: B20-B24.

Cases with mental disorders:

For patients with mental disorders, the following diagnoses were considered if present in the electronic health record:

- Psychiatric diagnosis: F00-F99, G30
- diagnosis before or within 3 months after the acquisition of the MRI scan;
- age >= 18 years at the time of the MRI scan;

Population B:

Non-psychiatric Controls:

Further exclusion criteria on Population A based on medication history. Specifically, we removed controls having brain medication utilizing the codes starting with N0[3-7], except for N05AD08 (Droperidol, anti-nausea medication) and N07BA01 (Nicotine, aid in quitting smoking).

Cases with mental disorders: Same as Population A.

Population C:

Non-psychiatric Controls: Same as Population B.

Cases with mental disorders:

Further exclusion criteria on Population B based on neurological medication history and neurological comorbidities:

- brain medication starting with N04.
- No neurological comorbidities:
    - Nervous system: G00-DG99, except G560 (Carpal tunnel syndrome) and G562 (Ulnar nerve neuropathy);
    - Cerebrovascular diagnosis: I60-69, E236E;
    - CNS infections: A022C, A066, A17, A229C, A321, A390, A504, A514B, A521A–B, A548A, A80–A89, B003–B004, B010–B011, B020–B021, B050–B051, B060, B261–B262, B375, B451, B582, B602, E236A;
    - Traumatic brain injury: S060-S069;
    - Skull fracture: S020, S021, S027, S029;
    - Malignant cancer: C00-C99;
    - Benign neoplasm in the nervous system: D32-D33;
    - HIV: B20-B24.

Supplementary Figure S1: Sensitivity analysis on the number of unique patients who received a diagnosis either before or after the MRI scan was taken, measured in months, and included patients who were diagnosed within 3 months before or after the date of the MRI (The results are based on the most inclusive criteria (Population A)).

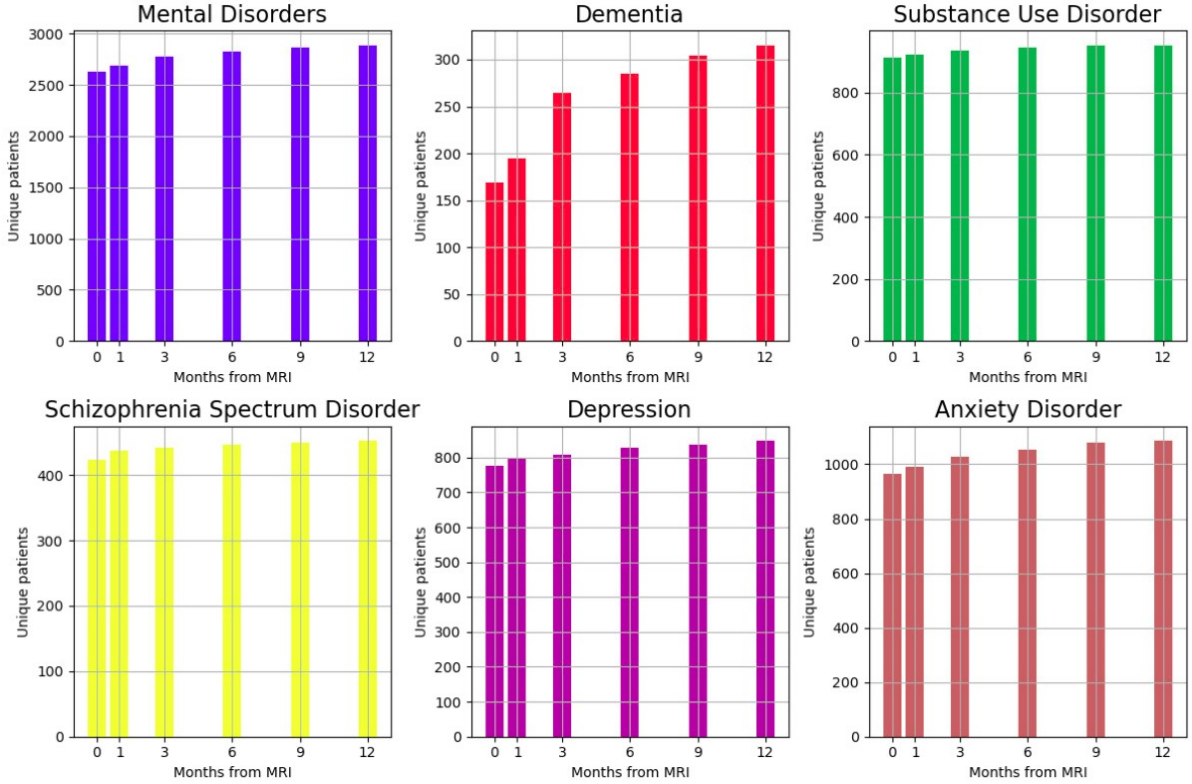

Supplementary Figure S2: Regions of interest. DK atlas parcellation[9] and recon-all-clinical whole-brain segmentation on "fsaverage" from FreeSurfer[10].

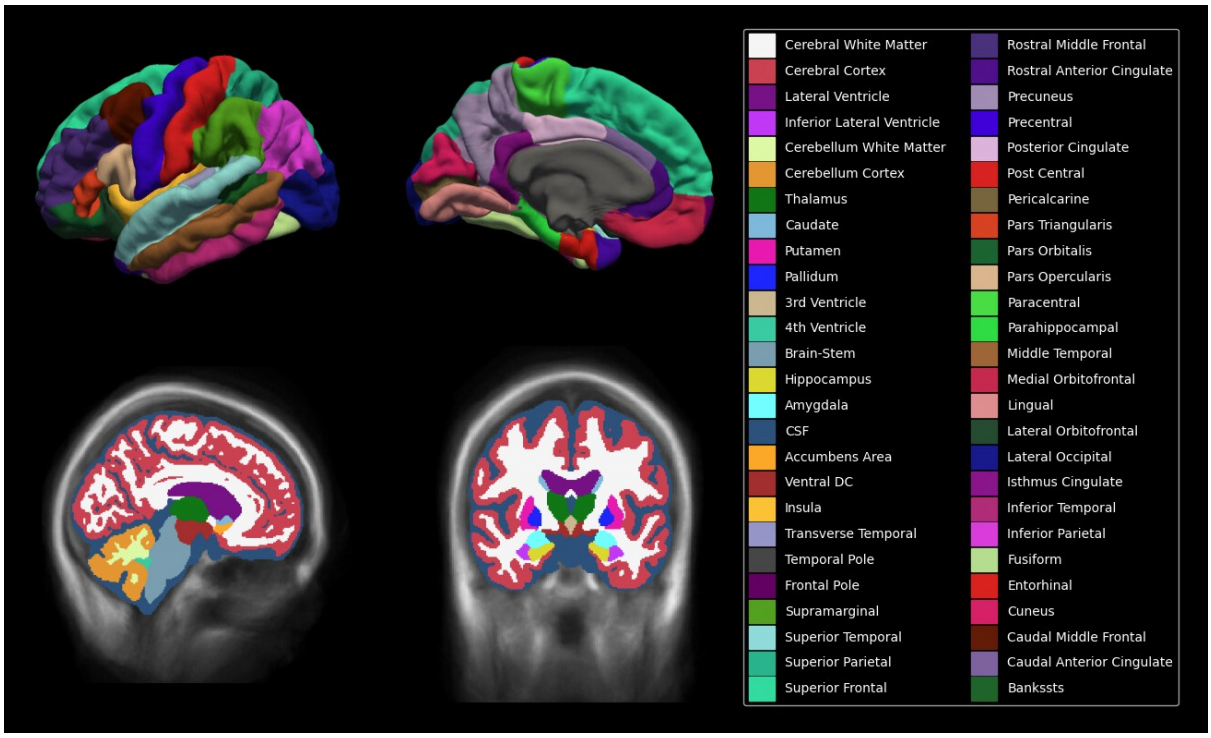

Supplementary Figure S3: MRI dataset information.

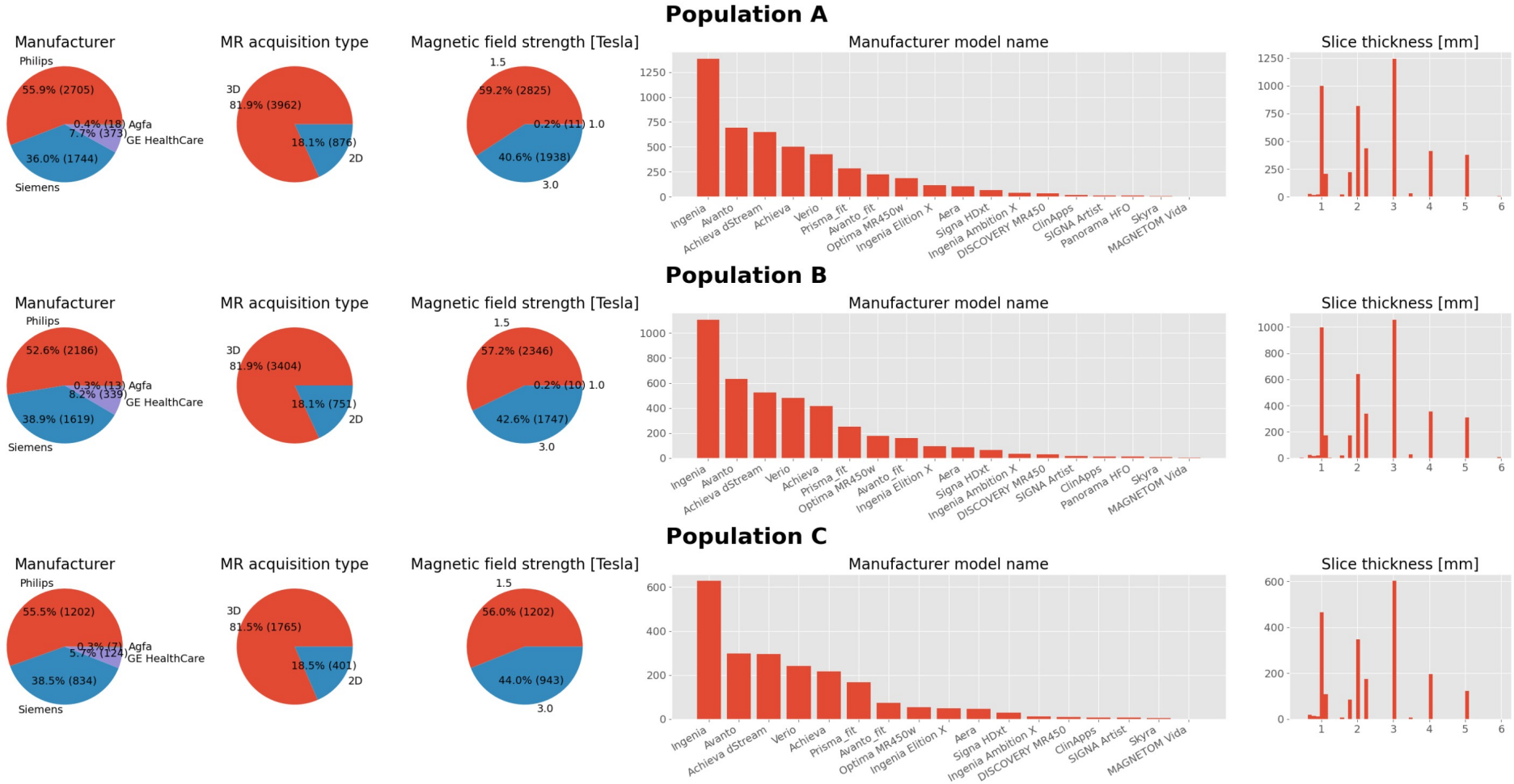

Supplementary Figure S4: Comparisons of all ROIs for Population A. Numerical values are provided in Supplementary Table S15.

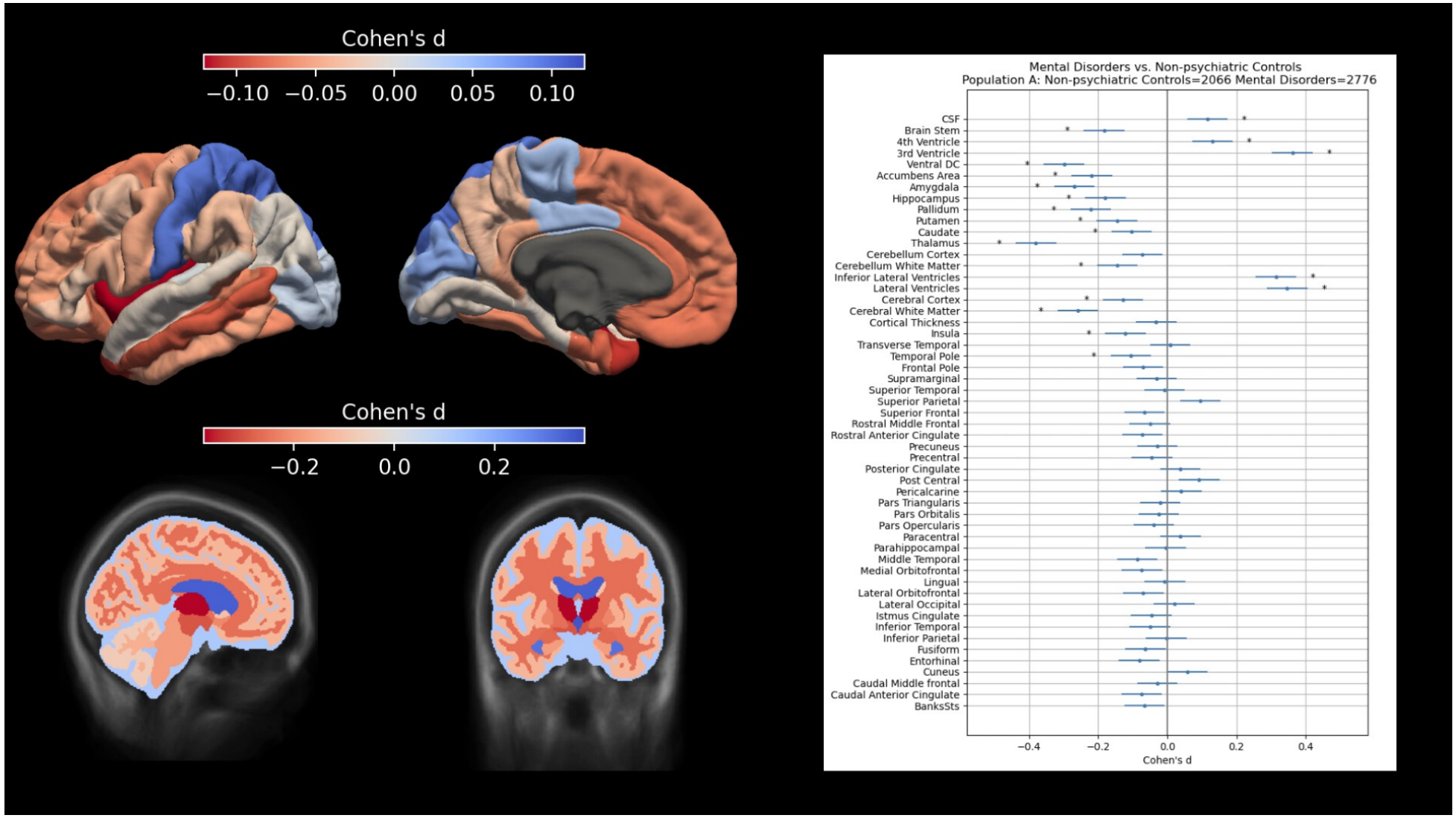

Supplementary Figure S5: Comparisons of all ROIs for Population B. Numerical values are provided in Supplementary Table S16.

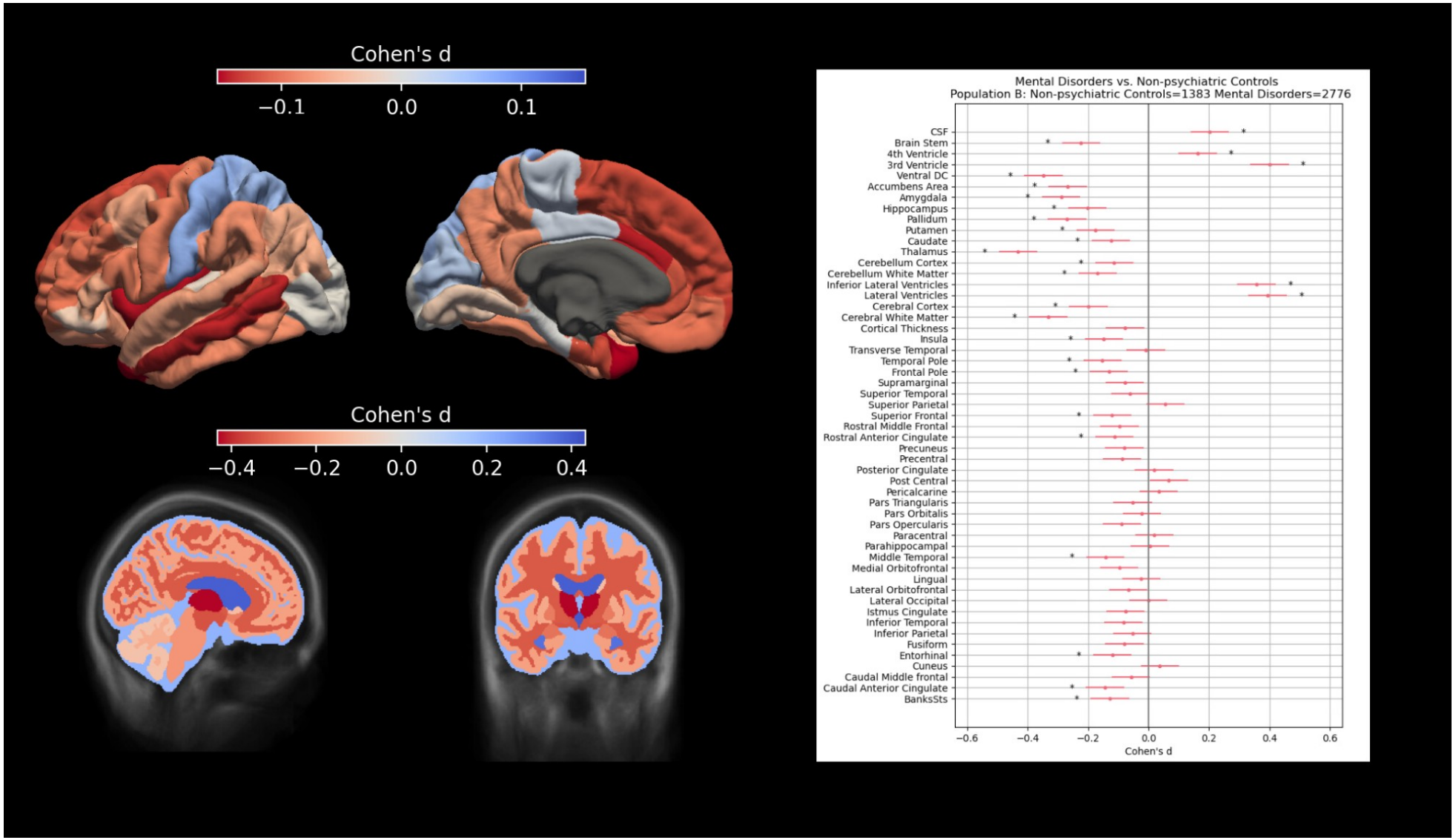

Supplementary Figure S6: Comparison of findings between mental disorders subgroups and controls, with prior ENIGMA studies for Population A. R=Right hemisphere, L=Left hemisphere, B=Bilateral. Numerical values are provided in Supplementary Table S18.

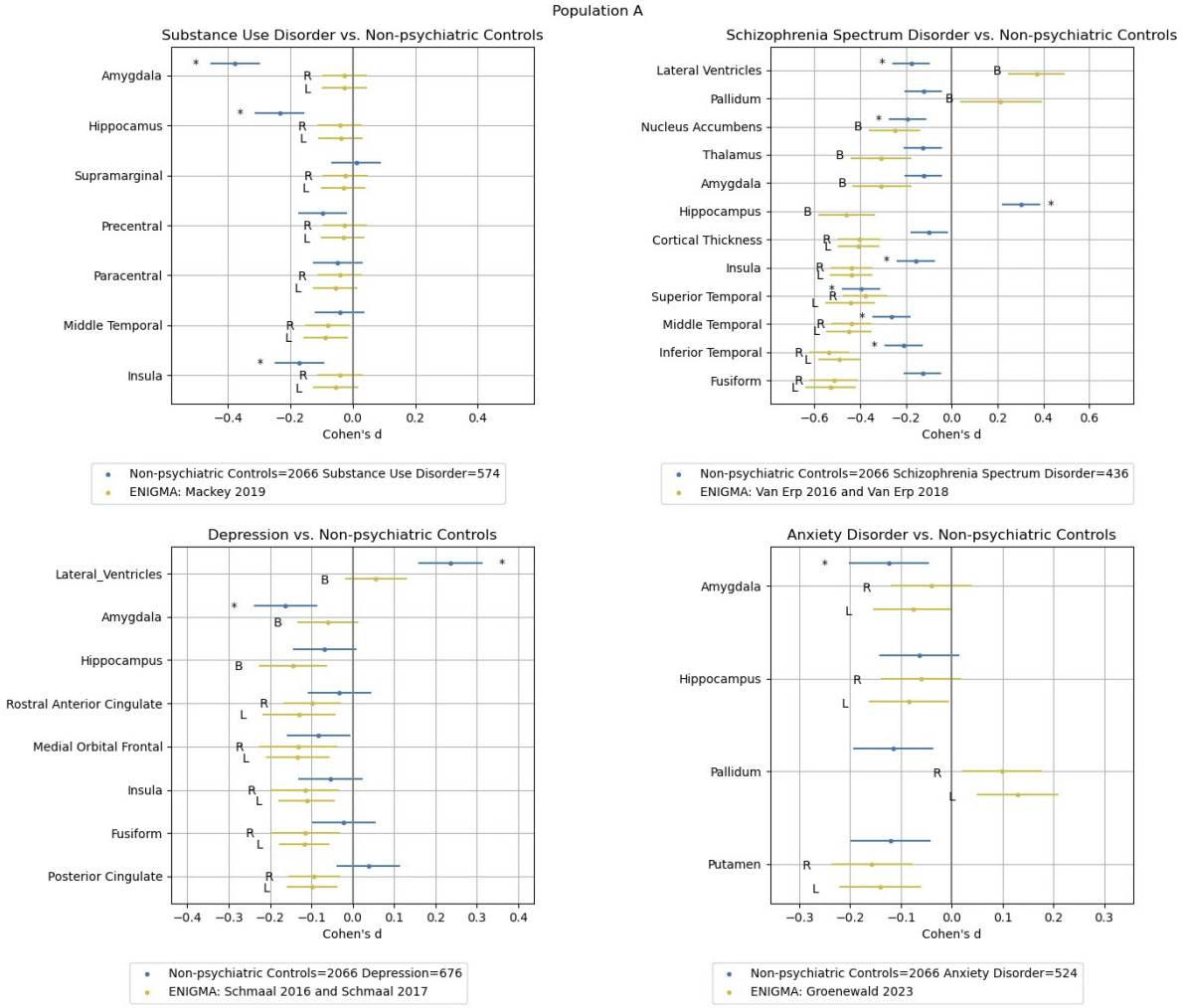

Supplementary Figure S7: Comparison of findings between mental disorders subgroups and controls, with prior ENIGMA studies for Population C. R=Right hemisphere, L=Left hemisphere, B=Bilateral. Numerical values are provided in Supplementary Table S20.

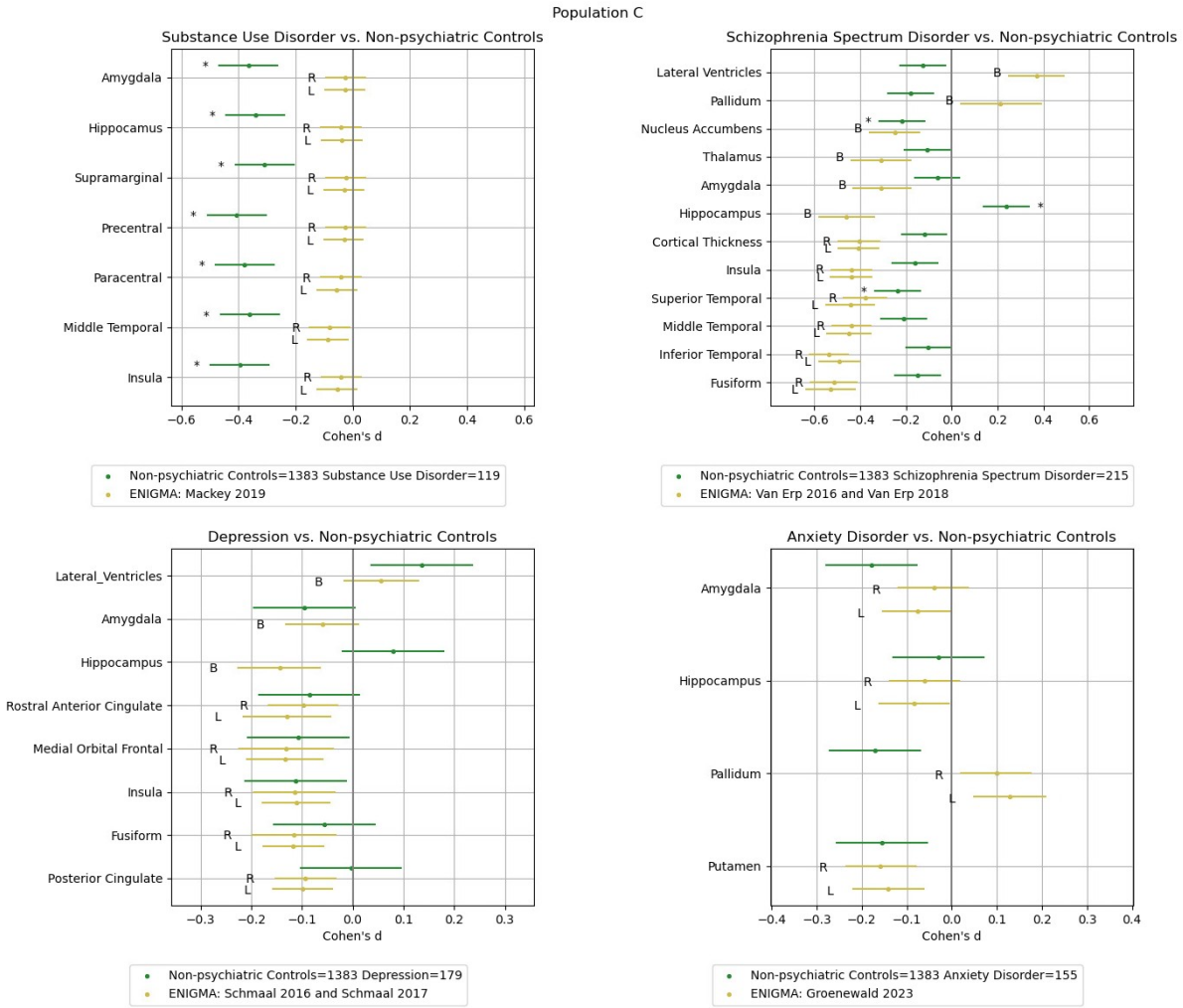

Supplementary Figure S8: Comparison of findings for high- (<1.5mm slice thickness) and low-resolution (>1.5mm slice thickness) scans for Population A and Population B. Numerical values are provided in Supplementary Table S12 and Table S13.

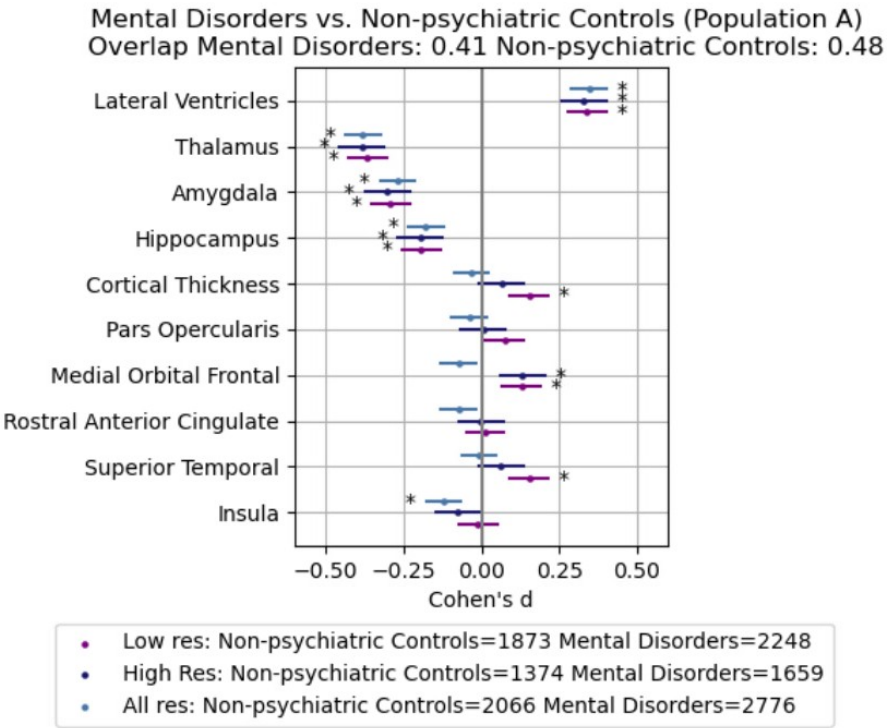

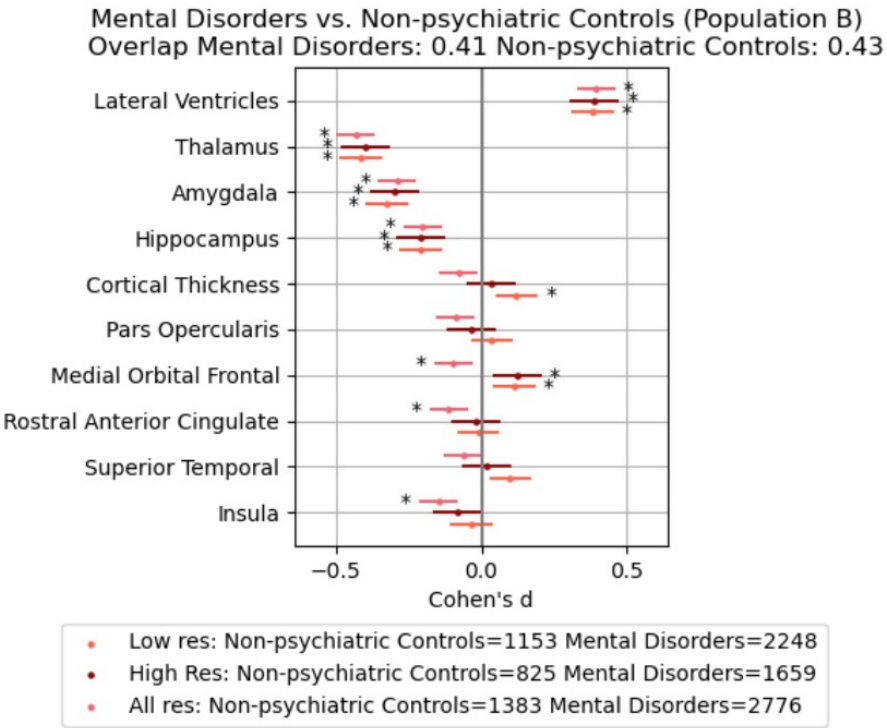

Supplementary Table S9: Comparison of mental disorders and dementia patients for previously reported ROI differences for Population A.

Population A	Cohen's d [95% CI]	p-value
Controls (N=2066) vs. Mental Disorders (N=2776)		
Lateral Ventricles	0.346 [0.290, 0.403]	2.66e-32 *
Thalamus	-0.380 [-0.437, -0.323]	1.88e-38 *
Amygdala	-0.269 [-0.326, -0.213]	2.92e-20 *
Hippocampus	-0.179 [-0.236, -0.123]	7.40e-10 *
Cortical Thickness	-0.032 [-0.089, 0.024]	2.64e-01
Pars Opercularis	-0.039 [-0.095, 0.017]	1.80e-01
Medial Orbitofrontal	-0.074 [-0.130, -0.017]	1.12e-02
Rostral Anterior Cingulate	-0.073 [-0.129, -0.017]	1.21e-02
Superior Temporal	-0.008 [-0.064, 0.048]	7.87e-01
Insula	-0.121 [-0.178, -0.065]	2.95e-05 *
Controls (N=2066) vs. Dementia (N=262)		
Lateral Ventricles	0.915 [0.830, 1.000]	1.57e-42 *
Hippocampus	-0.632 [-0.715, -0.549]	1.43e-21 *
Cortical Thickness	-0.299 [-0.380, -0.217]	5.49e-06 *
Entorhinal	-0.482 [-0.565, -0.400]	2.72e-13 *
Controls (N=2066) vs. Mental Disorders without Dementia (N=2608)		
Lateral Ventricles	0.314 [0.256, 0.372]	3.29e-26 *
Thalamus	-0.368 [-0.426, -0.310]	3.04e-35 *
Amygdala	-0.247 [-0.304, -0.189]	7.23e-17 *
Hippocampus	-0.158 [-0.216, -0.101]	8.16e-08 *
Cortical Thickness	-0.022 [-0.080, 0.035]	4.45e-01
Pars Opercularis	-0.032 [-0.089, 0.025]	2.76e-01
Medial Orbitofrontal	-0.065 [-0.123, -0.008]	2.68e-02
Rostral Anterior Cingulate	-0.065 [-0.123, -0.008]	2.69e-02
Superior Temporal	0.002 [-0.055, 0.059]	9.47e-01
Insula	-0.110 [-0.167, -0.052]	1.99e-04 *

Supplementary Table S10: Comparison of mental disorders and dementia patients for previously reported ROI differences for Population B.

Population B	Cohen's d [95% CI]	p-value
Controls (N=1383) vs. Mental Disorders (N=2776)		
Lateral Ventricles	0.394 [0.332, 0.455]	1.85e-32 *
Thalamus	-0.432 [-0.493, -0.370]	1.58e-38 *
Amygdala	-0.289 [-0.350, -0.228]	2.36e-18 *
Hippocampus	-0.202 [-0.263, -0.142]	8.41e-10 *
Cortical Thickness	-0.078 [-0.139, -0.017]	1.80e-02
Pars Opercularis	-0.089 [-0.150, -0.028]	6.92e-03
Medial Orbitofrontal	-0.097 [-0.158, -0.036]	3.27e-03 *
Rostral Anterior Cingulate	-0.113 [-0.174, -0.052]	6.16e-04 *
Superior Temporal	-0.062 [-0.122, -0.001]	6.13e-02
Insula	-0.148 [-0.209, -0.087]	7.18e-06 *
Controls (N=1383) vs. Dementia (N=262)		
Lateral Ventricles	1.048 [0.944, 1.151]	6.65e-51 *
Hippocampus	-0.681 [-0.780, -0.581]	2.64e-23 *
Cortical Thickness	-0.352 [-0.449, -0.254]	2.00e-07 *
Entorhinal	-0.591 [-0.690, -0.493]	4.23e-18 *
Controls (N=1383) vs. Mental Disorders without Dementia (N=2608)		
Lateral Ventricles	0.369 [0.306, 0.432]	3.55e-28 *
Thalamus	-0.421 [-0.484, -0.358]	4.88e-36 *
Amygdala	-0.271 [-0.333, -0.208]	5.45e-16 *
Hippocampus	-0.186 [-0.248, -0.123]	2.54e-08 *
Cortical Thickness	-0.069 [-0.131, -0.007]	3.78e-02
Pars Opercularis	-0.084 [-0.146, -0.022]	1.17e-02
Medial Orbitofrontal	-0.088 [-0.151, -0.026]	7.89e-03
Rostral Anterior Cingulate	-0.105 [-0.167, -0.043]	1.59e-03 *
Superior Temporal	-0.053 [-0.116, 0.009]	1.08e-01
Insula	-0.138 [-0.200, -0.076]	3.36e-05 *

Supplementary Table S11: Comparison of mental disorders and dementia patients for previously reported ROI differences for Population C.

Population C	Cohen's d [95% CI]	p-value
Controls (N=1383) vs. Mental Disorders (N=786)		
Lateral Ventricles	0.277 [0.193, 0.362]	6.37e-10 *
Thalamus	-0.303 [-0.387, -0.218]	1.60e-11 *
Amygdala	-0.245 [-0.329, -0.160]	4.92e-08 *
Hippocampus	-0.144 [-0.228, -0.059]	1.33e-03 *
Cortical Thickness	-0.207 [-0.291, -0.122]	4.00e-06 *
Pars Opercularis	-0.186 [-0.271, -0.102]	3.20e-05 *
Medial Orbitofrontal	-0.164 [-0.248, -0.079]	2.51e-04 *
Rostral Anterior Cingulate	-0.152 [-0.236, -0.067]	6.99e-04 *
Superior Temporal	-0.183 [-0.268, -0.099]	4.22e-05 *
Insula	-0.191 [-0.275, -0.106]	2.08e-05 *
Controls (N=1383) vs. Dementia (N=60)		
Lateral Ventricles	0.761 [0.654, 0.868]	9.84e-09 *
Hippocampus	-0.651 [-0.654, -0.868]	8.90e-07 *
Cortical Thickness	-0.663 [-0.769, -0.557]	5.64e-07 *
Entorhinal	-0.747 [-0.854, -0.640]	1.80e-08 *
Controls (N=1383) vs. Mental Disorders without Dementia (N=752)		
Lateral Ventricles	0.252 [0.167, 0.338]	2.85e-08 *
Thalamus	-0.285 [-0.371, -0.200]	3.68e-10 *
Amygdala	-0.210 [-0.295, -0.125]	3.70e-06 *
Hippocampus	-0.123 [-0.208, -0.038]	6.70e-03
Cortical Thickness	-0.184 [-0.269, -0.099]	4.95e-05 *
Pars Opercularis	-0.170 [-0.255, -0.085]	1.74e-04 *
Medial Orbitofrontal	-0.152 [-0.237, -0.067]	8.31e-04 *
Rostral Anterior Cingulate	-0.141 [-0.226, -0.056]	1.95e-03 *
Superior Temporal	-0.172 [-0.257, -0.087]	1.42e-04 *
Insula	-0.175 [-0.260, -0.090]	1.11e-04 *

Supplementary Table S12: Comparison of findings for high- (<1.5mm slice thickness) and low-resolution (≥1.5mm slice thickness) scans for Population A.

Population A. Overlap: Controls:% Mental Disorders:%	All Resolutions: Controls (N=2066) Mental Disorders (N=2776)		High Resolution: Controls (N=1374) Mental Disorders (N=1659)		Low Resolution: Controls (N=1873) Mental Disorders (N=2248)	
	Cohen's d [95% CI]	p-value	Cohen's d [95% CI]	p-value	Cohen's d [95% CI]	p-value
Lateral Ventricles	0.346 [0.290, 0.403]	2.66e-32 *	0.328 [0.256, 0.400]	4.23e-19 *	0.346 [0.290, 0.403]	2.66e-32 *
Thalamus	-0.380 [-0.437, -0.323]	1.88e-38 *	-0.385 [-0.456, -0.313]	1.50e-25 *	-0.367 [-0.328, -0.305]	3.04e-31 *
Amygdala	-0.269 [-0.326, -0.216]	2.92e-20 *	-0.303 [-0.375, -0.232]	1.38e-16 *	-0.293 [-0.354, -0.231]	1.33e-20 *
Hippocampus	-0.179 [-0.236, -0.123]	7.40e-10 *	-0.198 [-0.269, -0.126]	6.46e-08 *	-0.195 [-0.256, -0.133]	5.40e-10 *
Cortical Thickness	-0.032 [-0.089, 0.024]	2.64e-01	0.065 [-0.006, 0.137]	7.29e-02	0.153 [0.092, 0.214]	1.05e-06 *
Pars Opercularis	-0.039 [-0.095, 0.017]	1.80e-01	0.007 [-0.065, 0.078]	8.58e-01	0.075 [0.014, 0.136]	1.68e-02
Medial Orbitofrontal	-0.074 [-0.130, -0.017]	1.12e-02	0.131 [0.060, 0.202]	3.39e-04 *	0.130 [0.068, 0.191]	3.51e-05 *
Rostral Anterior Cingulate	-0.073 [-0.129, -0.017]	1.21e-02	-0.002 [-0.073, 0.069]	9.59e-01	0.012 [-0.049, 0.073]	7.04e-01
Superior Temporal	-0.008 [-0.064, 0.048]	7.87e-01	0.062 [-0.009, 0.134]	8.71e-02	0.153 [0.092, 0.214]	1.05e-06 *
Insula	-0.121 [-0.178, -0.065]	2.95e-05 *	-0.076 [-0.147, -0.005]	3.70e-02	-0.011 [-0.072, 0.050]	7.21e-01

Supplementary Table S13: Comparison of findings for high- (<1.5mm slice thickness) and low-resolution (≥1.5mm slice thickness) scans for Population B.

Population B. Overlap: Controls:% Mental Disorders:%	All Resolutions: Controls (N=1383) Mental Disorders (N=2776)		High Resolution: Controls (N=825) Mental Disorders (N=1659)		Low Resolution: Controls (N=1153) Mental Disorders (N=2248)	
	Cohen's d [95% CI]	p-value	Cohen's d [95% CI]	p-value	Cohen's d [95% CI]	p-value
Lateral Ventricles	0.394 [0.332, 0.455]	1.85e-32 *	0.388 [0.308, 0.467]	1.79e-19 *	0.480 [0.312, 0.448]	2.18e-25 *
Thalamus	-0.432 [-0.493, -0.370]	1.58e-38 *	-0.398 [-0.478, -0.319]	1.89e-20 *	-0.414 [-0.482, -0.346]	9.98e-30 *
Amygdala	-0.289 [-0.350, -0.228]	2.36e-18 *	-0.297 [-0.376, -0.218]	3.94e-12 *	-0.323 [-0.391, -0.256]	6.98e-19 *
Hippocampus	-0.202 [-0.263, -0.142]	8.41e-10 *	-0.207 [-0.286, -0.128]	1.22e-06 *	-0.209 [-0.276, -0.142]	8.55e-09 *
Cortical Thickness	-0.078 [-0.139, -0.017]	1.80e-02	0.036 [-0.043, 0.114]	4.03e-01	0.120 [0.053, 0.187]	9.41e-04 *
Pars Opercularis	-0.089 [-0.150, -0.028]	6.92e-03	-0.034 [-0.113, 0.044]	4.19e-01	0.036 [-0.032, 0.103]	3.27e-01
Medial Orbitofrontal	-0.097 [-0.158, -0.036]	3.27e-03 *	0.123 [0.044, 0.202]	3.87e-03 *	0.113 [0.046, 0.180]	1.80e-03 *
Rostral Anterior Cingulate	-0.113 [-0.174, -0.052]	6.16e-04 *	-0.020 [-0.099, 0.058]	6.33e-01	-0.011 [-0.078, 0.057]	7.70e-01
Superior Temporal	-0.062 [-0.122, -0.001]	6.13e-02	0.017 [-0.061, 0.096]	6.82e-01	0.099 [0.032, 0.166]	6.26e-03
Insula	-0.148 [-0.209, -0.087]	7.18e-06 *	-0.081 [-0.159, -0.002]	5.87e-02	-0.035 [-0.102, 0.032]	3.33e-01

Supplementary Table S14: Comparison of findings for high- (<1.5mm slice thickness) and low-resolution (≥1.5mm slice thickness) scans for Population C.

Population C. Overlap: Controls: 43.13% Mental Disorders: 39.19%	All Resolutions: Controls (N=1383) Mental Disorders (N=786)		High Resolution: Controls (N=825) Mental Disorders (N=483)		Low Resolution: Controls (N=1153) Mental Disorders (N=611)	
	Cohen's d [95% CI]	p-value	Cohen's d [95% CI]	p-value	Cohen's d [95% CI]	p-value
Lateral Ventricles	0.277 [0.193, 0.362]	6.37e-10 *	0.306 [0.196, 0.415]	1.14e-07 *	0.246 [0.152, 0.339]	9.97e-07 *
Thalamus	-0.303 [-0.387, -0.218]	1.60e-11 *	-0.257 [-0.366, -0.148]	8.08e-06 *	-0.299 [-0.393, -0.205]	2.74e-09 *
Amygdala	-0.245 [-0.329, -0.160]	4.92e-08 *	-0.281 [-0.390, -0.172]	1.10e-06 *	-0.279 [-0.372, -0.185]	2.98e-08 *
Hippocampus	-0.144 [-0.228, -0.059]	1.33e-03 *	-0.150 [-0.258, -0.041]	9.16e-03 *	-0.181 [-0.274, -0.087]	3.18e-04 *
Cortical Thickness	-0.207 [-0.291, -0.122]	4.00e-06 *	-0.112 [-0.211, -0.004]	5.01e-02	-0.041 [-0.135, 0.052]	4.11e-01
Pars Opercularis	-0.186 [-0.271, -0.102]	3.20e-05 *	-0.116 [-0.225, -0.008]	4.23e-02	-0.075 [-0.169, -0.018]	1.32e-01
Medial Orbitofrontal	-0.164 [-0.248, -0.079]	2.51e-04 *	0.042 [-0.066, 0.151]	4.61e-01	0.003 [-0.091, 0.096]	9.59e-01
Rostral Anterior Cingulate	-0.152 [-0.236, -0.067]	6.99e-04 *	-0.097 [-0.206, 0.011]	8.97e-02	-0.062 [-0.156, 0.031]	2.15e-01
Superior Temporal	-0.183 [-0.268, -0.099]	4.22e-05 *	-0.108 [-0.216, 0.001]	6.00e-02	-0.052 [-0.145, 0.042]	3.03e-01
Insula	-0.191 [-0.275, -0.106]	2.08e-05 *	-0.148 [-0.257, -0.040]	9.66e-03	-0.064 [-0.157, 0.030]	2.02e-01

Supplementary Table S15: Comparisons of all ROIs for Population A.

Population A	Cohen's d [95% CI]	p-value
Controls (N=2066) vs. Mental Disorders (N=2776)		
CSF	0.116 [0.059, 0.172]	6.77e-05 *
Brain Stem	-0.183 [-0.239, -0.126]	3.34e-10 *
4th Ventricle	0.130 [-0.074, 0.187]	7.46e-06 *
3rd Ventricle	0.362 [0.305, 0.419]	4.25e-35 *
Ventral DC	-0.299 [-0.356, -0.243]	1.31e-24 *
Nucleus Accumbens	-0.219 [-0.275, -0.162]	5.78e-14 *
Amygdala	-0.269 [-0.326, -0.213]	2.92e-20 *
Hippocampus	-0.179 [-0.236, -0.123]	7.40e-10 *
Pallidum	-0.222 [-0.278, -0.165]	2.64e-14 *
Putamen	-0.146 [-0.202, -0.089]	5.57e-07 *
Caudate	-0.103 [-0.160, -0.047]	3.77e-04 *
Thalamus	-0.380 [-0.437, -0.323]	1.88e-38 *
Cerebellum Cortex	-0.073 [-0.129, -0.017]	1.21e.02
Cerebellum White Matter	-0.144 [-0.201, -0.088]	6.88e-07 *
Inferior Lateral Ventricles	0.314 [0.257, 0.371]	6.97e-27 *
Lateral Ventricles	0.346 [0.290, 0.403]	2.66e-32 *
Cerebral Cortex	-0.128 [-0.184, -0.072]	1.06e-05 *
Cerebral White Matter	-0.259 [-0.316, -0.202]	6.87e-19 *
Cortical Thickness	-0.032 [-0.089, 0.024]	2.64e-01
Insula	-0.121 [-0.178, -0.065]	2.95e-05 *
Transverse Temporal	0.008 [-0.048, 0.065]	7.70e-01
Temporal Pole	-0.106 [-0.162, -0.050]	2.69e-04 *
Frontal Pole	-0.071 [-0.127, -0.015]	1.47e-02
Supramarginal	-0.031 [-0.087, 0.025]	2.86e-01
Superior Temporal	-0.008 [-0.064, 0.048]	7.87e-01
Superior Parietal	0.095 [0.039, 0.151]	1.07e-03
Superior Frontal	-0.066 [-0.123, -0.010]	2.25e-02
Rostral Middle Frontal	-0.051 [-0.107, 0.006]	8.19e-02
Rostral Anterior Cingulate	-0.073 [-0.129, -0.017]	1.21e-02
Precuneous	-0.029 [-0.085, 0.027]	3.18e-01
Precentral	-0.045 [-0.101, 0.012]	1.24e-01
Posterior Cingulate	0.037 [-0.019, 0.093]	2.04e-01
Post Central	0.092 [0.036, 0.148]	1.55e-03
Pericalcarine	0.040 [-0.016, 0.096]	1.67e-01
Pars Triangularis	-0.020 [-0.077, 0.036]	4.86e-01
Pars Orbitalis	-0.025 [-0.081, 0.031]	3.87e-01
Pars Opercularis	-0.039 [-0.095, 0.017]	1.80e-01
Paracentral	0.038 [-0.018, 0.095]	1.88e-01
Parahippocampal	-0.005 [-0.061, 0.051]	8.60e-01
Middle Temporal	-0.087 [-0.143, -0.031]	2.74e-03

Medial Orbitofrontal	-0.074 [-0.130, -0.017]	1.12e-02
Lingual	-0.007 [-0.064, 0.049]	7.99e-01
Lateral Orbitofrontal	-0.070 [-0.126, -0.013]	1.64e-02
Lateral Occipital	0.020 [-0.036, 0.076]	4.91e-01
Isthmus Cingulate	-0.046 [-0.103, 0.010]	1.10e-01
Inferior Temporal	-0.050 [-0.107, 0.006]	8.26e-02
Inferior Parietal	-0.003 [-0.059, 0.053]	9.17e-01
Fusiform	-0.064 [-0.120, -0.007]	2.87e-02
Entorhinal	-0.082 [-0.138, -0.025]	4.99e-03
Cuneous	0.057 [0.001, 0.113]	5.00e-02
Caudal Middle Frontal	-0.029 [-0.085, 0.027]	3.18e-01
Caudal Anterior Cingulate	-0.075 [-0.131, -0.019]	9.89e-03
BanksSts	-0.066 [-0.123, -0.010]	2.25e-02

Supplementary Table S16: Comparisons of all ROIs for Population B.

Population B	Cohen's d [95% CI]	p-value
Controls (N=1383) vs. Mental Disorders (N=2776)		
CSF	0.202 [0.141, 0.263]	9.65e-10 *
Brain Stem	-0.224 [-0.285, -0.163]	1.23e-11 *
4th Ventricle	0.162 [0.101, 0.223]	8.52e-07 *
3rd Ventricle	0.400 [0.338, 0.461]	2.15e-33 *
Ventral DC	-0.347 [-0.409, -0.286]	1.00e-25 *
Nucleus Accumbens	-0.268 [-0.329, -0.207]	5.57e-16 *
Amygdala	-0.289 [-0.350, -0.228]	2.36e-18 *
Hippocampus	-0.202 [-0.263, -0.142]	8.41e-10 *
Pallidum	-0.270 [-0.331, -0.209]	3.30e-16 *
Putamen	-0.176 [-0.236, -0.115]	1.01e-07 *
Caudate	-0.125 [-0.186, -0.064]	1.55e-04 *
Thalamus	-0.432 [-0.493, -0.370]	1.58e-38 *
Cerebellum Cortex	-0.114 [-0.174, -0.053]	5.69e-04 *
Cerebellum White Matter	-0.169 [-0.230, -0.108]	3.08e-07 *
Inferior Lateral Ventricles	0.357 [0.296, 0.419]	4.19e-27 *
Lateral Ventricles	0.394 [0.332, 0.455]	1.85e-32 *
Cerebral Cortex	-0.199 [-0.260, -0.138]	1.62e-09 *
Cerebral White Matter	-0.332 [-0.394, -0.271]	1.04e-23 *
Cortical Thickness	-0.078 [-0.139, -0.017]	1.80e-0e
Insula	-0.148 [-0.209, -0.087]	7.18e-06 *
Transverse Temporal	-0.009 [-0.070, 0.052]	7.78e-01
Temporal Pole	-0.153 [-0.214, -0.092]	3.45e-06 *
Frontal Pole	-0.131 [-0.192, -0.070]	7.26e-05 *
Supramarginal	-0.078 [-0.139, -0.017]	1.77e-02
Superior Temporal	-0.062 [-0.122, -0.001]	6.13e-02
Superior Parietal	0.056 [-0.005, 0.116]	9.08e-02
Superior Frontal	-0.121 [-0.182, -0.060]	2.47e-04 *
Rostral Middle Frontal	-0.096 [-0.157, -0.035]	3.57e-03
Rostral Anterior Cingulate	-0.113 [-0.174, -0.052]	6.16e-04 *
Precuneous	-0.080 [-0.141, -0.019]	1.49e-02
Precentral	-0.087 [-0.148, -0.027]	7.98e-03
Posterior Cingulate	0.018 [-0.042, 0.079]	5.77e-01
Post Central	0.067 [0.006, 0.128]	4.17e-02
Pericalcarine	0.033 [-0.028, 0.094]	3.13e-01
Pars Triangularis	-0.053 [-0.114, 0.008]	1.09e-01
Pars Orbitalis	-0.022 [-0.083, 0.039]	5.00e-01
Pars Opercularis	-0.089 [-0.150, -0.028]	6.92e-03
Paracentral	0.018 [-0.042, 0.079]	5.74e-01
Parahippocampal	0.005 [-0.056, 0.065]	8.88e-01
Middle Temporal	-0.142[-0.203, -0.081]	1.59e-05 *

Medial Orbitofrontal	-0.097 [-0.158, -0.036]	3.27e-03
Lingual	-0.025 [-0.086, 0.036]	4.52e-01
Lateral Orbitofrontal	-0.067 [-0.128, -0.007]	4.07e-02
Lateral Occipital	-0.001 [-0.062, 0.060]	9.81e-01
Isthmus Cingulate	-0.076 [-0.137, -0.015]	2.10e-02
Inferior Temporal	-0.083 [-0.144, -0.023]	1.13e-02
Inferior Parietal	-0.053 [-0.114, 0.008]	1.08e-01
Fusiform	-0.080 [-0.141, 0.019]	1.48e-02
Entorhinal	-0.120 [-0.180, -0.059]	2.85e-04 *
Cuneous	0.037 [-0.024, 0.098]	2.60e-01
Caudal Middle Frontal	-0.058 [-0.119, 0.003]	7.89e-02
Caudal Anterior Cingulate	-0.144 [-0.205, -0.083]	1.22e-05 *
BanksSts	-0.128 [-0.189, -0.067]	1.01e-04 *

Supplementary Table S17: Comparisons of all ROIs for Population C.

Population C	Cohen's d [95% CI]	p-value
Controls (N=1383) vs. Mental Disorders (N=786)		
CSF	0.268 [0.183, 0.353]	2.30e-09 *
Brain Stem	-0.149 [-0.233, -0.064]	8.99e-04 *
4th Ventricle	0.057 [-0.027, 0.141]	2.03e-01
3rd Ventricle	0.320 [0.236, 0.405]	1.02e-12 *
Ventral DC	-0.224 [-0.308, -0.139]	6.01e-07 *
Nucleus Accumbens	-0.179 [-0.264, -0.095]	6.21e-05 *
Amygdala	-0.245 [-0.329, -0.160]	4.92e-08 *
Hippocampus	-0.144 [-0.228, -0.059]	1.33e-03
Pallidum	-0.175 [-0.260, -0.091]	8.86e-05 *
Putamen	-0.073 [-0.158, 0.011]	1.01e-01
Caudate	-0.097 [-0.181, -0.013]	2.96e-02
Thalamus	-0.303 [-0.387, -0.218]	1.60e-11 *
Cerebellum Cortex	-0.153 [-0.238, -0.069]	6.04e-04 *
Cerebellum White Matter	-0.151 [-0.236, -0.067]	7.20e-04 *
Inferior Lateral Ventricles	0.363 [0.278, 0.448]	7.75e-16 *
Lateral Ventricles	0.277 [0.193, 0.362]	6.37e-10 *
Cerebral Cortex	-0.236 [-0.321, -0.152]	1.34e-07 *
Cerebral White Matter	-0.256 [-0.341, -0.172]	1.09e-08 *
Cortical Thickness	-0.207 [-0.291, -0.122]	4.00e-06 *
Insula	-0.191 [-0.275, -0.106]	2.08e-05 *
Transverse Temporal	-0.111 [-0.195, -0.027]	1.30e-02
Temporal Pole	-0.241 [-0.326, -0.157]	7.38e-08 *
Frontal Pole	-0.210 [-0.295, -0.126]	2.67e-06 *
Supramarginal	-0.173 [-0.258, -0.089]	1.08e-04 *
Superior Temporal	-0.183 [-0.268, -0.099]	4.22e-05 *
Superior Parietal	-0.079 [-0.164, 0.005]	7.61e-02
Superior Frontal	-0.229 [-0.313, -0.144]	3.40e-07 *
Rostral Middle Frontal	-0.210 [-0.294, -0.125]	2.82e-06 *
Rostral Anterior Cingulate	-0.152 [-0.236, -0.067]	6.99e-04 *
Precuneous	-0.205 [-0.290, -0.121]	4.47e-06 *
Precentral	-0.152 [-0.237, -0.068]	6.57e-04 *
Posterior Cingulate	-0.067 [-0.151, 0.018]	1.37e-01
Post Central	-0.073 [-0.157, 0.012]	1.04e-01
Pericalcarine	-0.054 [-0.138, 0.031]	2.30e-01
Pars Triangularis	-0.159 [-0.243, -0.075]	3.82e-04 *
Pars Orbitalis	-0.105 [-0.189, -0.021]	1.90e-02
Pars Opercularis	-0.186 [-0.271, -0.102]	3.20e-05 *
Paracentral	-0.079 [-0.163, 0.005]	7.70e-02
Parahippocampal	-0.019 [-0.103, 0.066]	6.78e-01
Middle Temporal	-0.242 [-0.327, -0.157]	6.72e-08 *

Medial Orbitofrontal	-0.164 [-0.248, -0.079]	2.51e-04 *
Lingual	-0.159 [-0.244, -0.075]	3.70e-04 *
Lateral Orbitofrontal	-0.133 [-0.217, -0.048]	2.99e-03
Lateral Occipital	-0.131 [-0.215, -0.046]	3.50e-03
Isthmus Cingulate	-0.190 [-0.274, -0.106]	2.21e-05 *
Inferior Temporal	-0.160 [-0.244, -0.076]	3.50e-04 *
Inferior Parietal	-0.176 [-0.260, -0.091]	8.80e-05 *
Fusiform	-0.185 [-0.269, -0.101]	3.62e-05 *
Entorhinal	-0.183 [-0.267, -0.098]	4.42e-05 *
Cuneous	-0.089 [-0.173, -0.004]	4.72e-02
Caudal Middle Frontal	-0.155 [-0.240, -0.071]	5.24e-04 *
Caudal Anterior Cingulate	-0.170 [-0.254, -0.086]	1.47e-04 *
BanksSts	-0.192 [-0.276, -0.107]	1.86e-05 *

Supplementary Table S18: Comparison of findings between mental disorders subgroups and controls, with prior ENIGMA studies for Population A. R=Right hemisphere, L=Left hemisphere, B=Bilateral.

Population A	Cohen's d [95% CI]	p-value	ENIGMA studies: Cohen's d [95% CI] [Reference]
Controls (N=2066) vs. Substance Use Disorder (N=574)			
Amygdala	-0.377 [-0.454, -0.300]	2.03e-15 *	R: -0.041 [-0.110, 0.028] L: -0.055 [-0.124, 0.014] [11]
Hippocampus	-0.234 [-0.311, -0.158]	7.30e-07 *	R: -0.081 [-0.150, -0.012] L: -0.087 [-0.156, -0.018] [11]
Insula	-0.172 [-0.248, 0.095]	2.82e-04 *	R: -0.042 [-0.111, 0.027] L: -0.056 [-0.125, 0.013] [11]
Middle Temporal	-0.042 [-0.118, 0.034]	3.72e-01	R: -0.026 [-0.095, 0.043] L: -0.030 [-0.099, 0.034] [11]
Paracentral	-0.049 [-0.125, 0.028]	3.03e-01	R: -0.024 [-0.093, 0.045] L: -0.031 [-0.100, 0.038] [11]
Precentral	-0.096 [-0.173, -0.020]	4.10e-02	R: -0.042 [-0.111, 0.027] L: -0.039 [-0.108, 0.030] [11]
Supramarginal	0.012 [-0.065, 0.088]	8.05e-01	R: -0.026 [-0.095, 0.043] L: -0.027 [-0.096, 0.042] [11]
Controls (N=2066) vs. Schizophrenia Spectrum Disorder (N=436)			
Hippocampus	0.304 [0.225, 0.383]	9.21e-09 *	B: -0.46 [-0.58, -0.34] [12]
Amygdala	-0.124 [-0.203, -0.046]	1.85e-02	B: -0.31 [-0.43, -0.18] [12]
Thalamus	-0.127 [-0.206, -0.049]	1.60e-02	B: -0.31 [-0.44, -0.18] [12]
Nucleus Accumbens	-0.193 [-0.272, -0.115]	2.50e-04 *	B: -0.25 [-0.36, -0.14] [12]
Pallidum	-0.124 [-0.203, -0.046]	1.84e-02	B: 0.21 [0.04, 0.39] [12]
Lateral Ventricles	-0.177 [-0.256, -0.099]	7.74e-04 *	B: 0.37 [0.25, 0.49] [12]
Cortical Thickness	-0.098 [-0.177, -0.020]	6.22e-02	R: -0.516 [-0.618, -0.414] L: -0.530 [-0.637, -0.423] [13]
Fusiform	-0.128 [-0.207, -0.050]	1.52e-02	R: -0.536 [-0.62, -0.452] L: -0.491 [-0.579, -0.403] [13]
Inferior Temporal	-0.211 [-0.290, -0.132]	6.44e-05 *	R: -0.439 [-0.522, -0.355] L: -0.449 [-0.543, -0.356] [13]
Middle Temporal	-0.263 [-0.342, -0.184]	6.57e-07 *	R: -0.379 [-0.472, -0.286] L: -0.444 [-0.549, -0.339] [13]
Superior Temporal	-0.398 [-0.477, -0.319]	6.20e-14 *	R: -0.438 [-0.526, -0.351] L: -0.440 [-0.529, -0.352] [13]
Insula	-0.158 [-0.236, -0.079]	2.83e-03 *	R: -0.406 [-0.497, -0.315] L: -0.408 [-0.494, -0.322] [13]
Controls (N=2066) vs. Depression (N=676)			
Hippocampus	-0.068 [-0.143, 0.007]	1.26e-01	B: -0.144 [-0.225, -0.064] [14]
Amygdala	-0.163 [-0.238, -0.088]	2.44e-04 *	B: -0.060 [-0.132, 0.011] [14]
Lateral Ventricles	0.236 [0.161, 0.311]	1.07e-07 *	B: 0.056 [-0.017, 0.129] [14]
Posterior Cingulate	0.038 [-0.037, 0.113]	3.93e-01	R: -0.093 [-0.152, -0.034] L: -0.099 [-0.158, -0.040] [15]

Fusiform	-0.021 [-0.096, 0.053]	6.29e-01	R: -0.116 [-0.198, -0.033] L: -0.117 [-0.176, -0.058] [15]
Insula	-0.054 [-0.129, 0.021]	2.25e-01	R: -0.115 [-0.195, -0.035] L: -0.111 [-0.177, -0.045] [15]
Medial Orbitofrontal	-0.083 [-0.158, -0.008]	6.11e-02	R: -0.131 [-0.224, -0.039] L: -0.134 [-0.208, -0.059] [15]
Rostral Anterior Cingulate	-0.033 [-0.107, 0.042]	4.62e-01	R: -0.098 [-0.165, -0.031] L: -0.130 [-0.216, -0.044] [15]
Controls (N=2066) vs. Anxiety Disorder (N=524)			
Putamen	-0.121 [-0.198, -0.044]	1.34e-02	R: -0.158 [-0.235, -0.080] L: -0.141 [-0.219, -0.062] [16]
Pallidum	-0.115 [-0.192, -0.038]	1.85e-02	R: 0.099 [0.021, 0.176] L: 0.129 [0.050, 0.208] [16]
Hippocampus	-0.063 [-0.140, 0.014]	1.96e-01	R: -0.060 [-0.137, 0.016] L: -0.084 [-0.161, -0.007] [16]
Amygdala	-0.123 [-0.200, -0.046]	1.17e-02 *	R: -0.040 [-0.118, 0.037] L: -0.076 [-0.153, -0.001] [16]

Supplementary Table S19: Comparison of findings between mental disorders subgroups and controls, with prior ENIGMA studies for Population B. R=Right hemisphere, L=Left hemisphere, B=Bilateral.

Population B	Cohen's d [95% CI]	p-value	ENIGMA studies: Cohen's d [95% CI] [Reference]
Controls (N=1383) vs. Substance Use Disorder (N=574)			
Amygdala	-0.401 [-0.491, -0.312]	1.13e-15 *	R: -0.041 [-0.110, 0.028] L: -0.055 [-0.124, 0.014] [11]
Hippocampus	-0.272 [-0.361, -0.183]	4.76e-08 *	R: -0.081 [-0.150, -0.012] L: -0.087 [-0.156, -0.018] [11]
Insula	-0.197 [-0.286, -0.108]	7.72e-05 *	R: -0.042 [-0.111, 0.027] L: -0.056 [-0.125, 0.013] [11]
Middle Temporal	-0.093 [-0.182, -0.004]	6.08e-02	R: -0.026 [-0.095, 0.043] L: -0.030 [-0.099, 0.034] [11]
Paracentral	-0.071 [-0.160, 0.017]	1.51e-01	R: -0.024 [-0.093, 0.045] L: -0.031 [-0.100, 0.038] [11]
Precentral	-0.130 [-0.219, -0.042]	8.66e-03	R: -0.042 [-0.111, 0.027] L: -0.039 [-0.108, 0.030] [11]
Supramarginal	-0.029 [-0.117, 0.060]	5.63e-01	R: -0.026 [-0.095, 0.043] L: -0.027 [-0.096, 0.042] [11]
Controls (N=1383) vs. Schizophrenia Spectrum Disorder (N=436)			
Hippocampus	0.365 [0.272, 0.458]	4.10e-11 *	B: -0.46 [-0.58, -0.34] [12]
Amygdala	-0.058 [-0.150, 0.034]	2.89e-01	B: -0.31 [-0.43, -0.18] [12]
Thalamus	-0.074 [-0.166, 0.018]	1.79e-01	B: -0.31 [-0.44, -0.18] [12]
Nucleus Accumbens	-0.179 [-0.271, -0.086]	1.16e-03 *	B: -0.25 [-0.36, -0.14] [12]
Pallidum	-0.120 [-0.212, -0.028]	2.91e-02	B: 0.21 [0.04, 0.39] [12]
Lateral Ventricles	-0.169 [-0.261, -0.077]	2.15e-03 *	B: 0.37 [0.25, 0.49] [12]
Cortical Thickness	-0.167 [-0.259, -0.075]	2.42e-03 *	R: -0.516 [-0.618, -0.414] L: -0.530 [-0.637, -0.423] [13]
Fusiform	-0.096 [-0.188, -0.004]	8.18e-02	R: -0.536 [-0.62, -0.452] L: -0.491 [-0.579, -0.403] [13]
Inferior Temporal	-0.211 [-0.303, -0.119]	1.27e-04 *	R: -0.439 [-0.522, -0.355] L: -0.449 [-0.543, -0.356] [13]
Middle Temporal	-0.275 [-0.368, -0.183]	5.94e-07 *	R: -0.379 [-0.472, -0.286] L: -0.444 [-0.549, -0.339] [13]
Superior Temporal	-0.418 [-0.511, -0.326]	4.11e-14 *	R: -0.438 [-0.526, -0.351] L: -0.440 [-0.529, -0.352] [13]
Insula	-0.225 [-0.317, -0.133]	4.46e-05 *	R: -0.406 [-0.497, -0.315] L: -0.408 [-0.494, -0.322] [13]
Controls (N=1383) vs. Depression (N=676)			
Hippocampus	-0.097 [-0.183, -0.010]	3.97e-02	B: -0.144 [-0.225, -0.064] [14]
Amygdala	-0.205 [-0.291, -0.118]	1.34e-05 *	B: -0.060 [-0.132, 0.011] [14]
Lateral Ventricles	0.311 [0.224, 0.398]	4.18e-11 *	B: 0.056 [-0.017, 0.129] [14]
Posterior Cingulate	0.038 [-0.048, 0.125]	4.13e-01	R: -0.093 [-0.152, -0.034] L: -0.099 [-0.158, -0.040] [15]
Fusiform	-0.020 [-0.107, 0.066]	6.68e-01	R: -0.116 [-0.198, -0.033] L: -0.117 [-0.176, -0.058] [15]

Insula	-0.069 [-0.155, 0.018]	1.44e-01	R: -0.115 [-0.195, -0.035] L: -0.111 [-0.177, -0.045] [15]
Medial Orbitofrontal	-0.080 [-0.166, 0.007]	8.93e-02	R: -0.131 [-0.224, -0.039] L: -0.134 [-0.208, -0.059] [15]
Rostral Anterior Cingulate	-0.065 [-0.151, 0.022]	1.68e-01	R: -0.098 [-0.165, -0.031] L: -0.130 [-0.216, -0.044] [15]
Controls (N=1383) vs. Anxiety Disorder (N=524)			
Putamen	-0.174 [-0.264, -0.084]	6.86e-04 *	R: -0.158 [-0.235, -0.080] L: -0.141 [-0.219, -0.062] [16]
Pallidum	-0.208 [-0.298, -0.118]	5.37e-05 *	R: 0.099 [0.021, 0.176] L: 0.129 [0.050, 0.208] [16]
Hippocampus	-0.116 [-0.206, -0.027]	2.34e-02	R: -0.060 [-0.137, 0.016] L: -0.084 [-0.161, -0.007] [16]
Amygdala	-0.176 [-0.266, -0.086]	6.17e-04 *	R: -0.040 [-0.118, 0.037] L: -0.076 [-0.153, -0.001] [16]

Supplementary Table S20: Comparison of findings between mental disorders subgroups and controls, with prior ENIGMA studies for Population C. R=Right hemisphere, L=Left hemisphere, B=Bilateral.

Population C	Cohen's d [95% CI]	p-value	ENIGMA studies: Cohen's d [95% CI] [Reference]
Controls (N=1383) vs. Substance Use Disorder (N=119)			
Amygdala	-0.365 [-0.467, -0.263]	1.38e-04 *	R: -0.041 [-0.110, 0.028] L: -0.055 [-0.124, 0.014] [11]
Hippocampus	-0.341 [-0.443, -0.239]	3.68e-04 *	R: -0.081 [-0.150, -0.012] L: -0.087 [-0.156, -0.018] [11]
Insula	-0.396 [-0.498, -0.293]	3.66e-05 *	R: -0.042 [-0.111, 0.027] L: -0.056 [-0.125, 0.013] [11]
Middle Temporal	-0.361 [-0.463, -0.259]	1.66e-04 *	R: -0.026 [-0.095, 0.043] L: -0.030 [-0.099, 0.034] [11]
Paracentral	-0.378 [-0.481, -0.276]	7.80e-05 *	R: -0.024 [-0.093, 0.045] L: -0.031 [-0.100, 0.038] [11]
Precentral	-0.406 [-0.508, -0.304]	2.27e-05 *	R: -0.042 [-0.111, 0.027] L: -0.039 [-0.108, 0.030] [11]
Supramarginal	-0.309 [-0.411, -0.207]	1.25e-03 *	R: -0.026 [-0.095, 0.043] L: -0.027 [-0.096, 0.042] [11]
Controls (N=1383) vs. Schizophrenia Spectrum Disorder (N=215)			
Hippocampus	0.239 [0.140, 0.337]	1.14e-03 *	B: -0.46 [-0.58, -0.34] [12]
Amygdala	-0.064 [-0.162, 0.034]	3.84e-01	B: -0.31 [-0.43, -0.18] [12]
Thalamus	-0.107 [-0.205, -0.009]	1.45e-01	B: -0.31 [-0.44, -0.18] [12]
Nucleus Accumbens	-0.218 [-0.316, -0.119]	3.05e-03 *	B: -0.25 [-0.36, -0.14] [12]
Pallidum	-0.181 [-0.279, -0.082]	1.39e-02	B: 0.21 [0.04, 0.39] [12]
Lateral Ventricles	-0.125 [-0.224, -0.027]	8.71e-02	B: 0.37 [0.25, 0.49] [12]
Cortical Thickness	-0.121 [-0.219, -0.022]	1.00e-01	R: -0.516 [-0.618, -0.414] L: -0.530 [-0.637, -0.423] [13]
Fusiform	-0.151 [-0.249, -0.052]	4.01e-01	R: -0.536 [-0.62, -0.452] L: -0.491 [-0.579, -0.403] [13]
Inferior Temporal	-0.102 [-0.200, -0.004]	1.64e-01	R: -0.439 [-0.522, -0.355] L: -0.449 [-0.543, -0.356] [13]
Middle Temporal	-0.210 [-0.309, -0.112]	4.21e-03	R: -0.379 [-0.472, -0.286] L: -0.444 [-0.549, -0.339] [13]
Superior Temporal	-0.238 [-0.336, -0.139]	1.20e-03 *	R: -0.438 [-0.526, -0.351] L: -0.440 [-0.529, -0.352] [13]
Insula	-0.161 [-0.259, -0.063]	2.83e-02	R: -0.406 [-0.497, -0.315] L: -0.408 [-0.494, -0.322] [13]
Controls (N=1383) vs. Depression (N=179)			
Hippocampus	0.079 [-0.020, 0.179]	3.18e-01	B: -0.144 [-0.225, -0.064] [14]
Amygdala	-0.095 [-0.195, 0.004]	2.31e-01	B: -0.060 [-0.132, 0.011] [14]
Lateral Ventricles	0.135 [0.036, 0.235]	8.84e-02	B: 0.056 [-0.017, 0.129] [14]
Posterior Cingulate	-0.004 [-0.103, 0.096]	9.63e-01	R: -0.093 [-0.152, -0.034] L: -0.099 [-0.158, -0.040] [15]
Fusiform	-0.057 [-0.156, 0.043]	4.76e-01	R: -0.116 [-0.198, -0.033] L: -0.117 [-0.176, -0.058] [15]

Insula	-0.113 [-0.212, -0.014]	1.55e-01	R: -0.115 [-0.195, -0.035] L: -0.111 [-0.177, -0.045] [15]
Medial Orbitofrontal	-0.107 [-0.207, -0.008]	1.77e-01	R: -0.131 [-0.224, -0.039] L: -0.134 [-0.208, -0.059] [15]
Rostral Anterior Cingulate	-0.086 [-0.185, 0.013]	2.80e-01	R: -0.098 [-0.165, -0.031] L: -0.130 [-0.216, -0.044] [15]
Controls (N=1383) vs. Anxiety Disorder (N=155)			
Putamen	-0.155 [-0.255, -0.054]	6.81e-02	R: -0.158 [-0.235, -0.080] L: -0.141 [-0.219, -0.062] [16]
Pallidum	-0.171 [-0.271, -0.071]	4.37e-02	R: 0.099 [0.021, 0.176] L: 0.129 [0.050, 0.208] [16]
Hippocampus	-0.030 [-0.130, 0.07]	7.25e-01	R: -0.060 [-0.137, 0.016] L: -0.084 [-0.161, -0.007] [16]
Amygdala	-0.178 [-0.279, -0.078]	3.54e-02	R: -0.040 [-0.118, 0.037] L: -0.076 [-0.153, -0.001] [16]

References:

1. Chen, T., & Guestrin, C. (2016). Xgboost: A scalable tree boosting system. In Proceedings of the 22nd acm sigkdd international conference on knowledge discovery and data mining (pp. 785-794).

2. Li, X., Morgan, P. S., Ashburner, J., Smith, J., & Rorden, C. (2016). The first step for neuroimaging data analysis: DICOM to NIfTI conversion. Journal of neuroscience methods, 264, 47-56.

3. Gopinath, K., Greve, D. N., Das, S., Arnold, S., Magdamo, C., & Iglesias, J. E. (2023). Cortical analysis of heterogeneous clinical brain MRI scans for large-scale neuroimaging studies. In International Conference on Medical Image Computing and Computer-Assisted Intervention, pages 35–45. Springer.

4. Billot, B., Greve, D. N., Puonti, O., Thielscher, A., Van Leemput, K., Fischl, B., Dalca, A. V., Iglesias, J. E., et al. (2023a). SynthSeg: Segmentation of brain MRI scans of any contrast and resolution without retraining. Medical image analysis, 86:102789.

5. Billot, B., Magdamo, C., Cheng, Y., Arnold, S. E., Das, S., and Iglesias, J. E. (2023b). Robust machine learning segmentation for large-scale analysis of heterogeneous clinical brain MRI datasets. Proceedings of the National Academy of Sciences, 120(9):e2216399120.

6. Iglesias, J. E., Billot, B., Balbastre, Y., Magdamo, C., Arnold, S. E., Das, S., Edlow, B. L., Alexander, D. C., Golland, P., and Fischl, B. (2023). SynthSR: A public AI tool to turn heterogeneous clinical brain scans into high-resolution T1-weighted images for 3D morphometry. Science advances, 9(5):eadd3607.

7. Dice, L. R. (1945). Measures of the amount of ecologic association between species. Ecology, 26(3), 297-302.

8. https://icd.who.int/browse10/2019/en

9. Desikan, R. S., Segonne, F., Fischl, B., Quinn, B. T., Dickerson, B. C., Blacker, D., Buckner, R. L., Dale, A. M., Maguire, R. P., Hyman, B. T., et al. (2006). An automated labeling system for subdividing the human cerebral cortex on MRI scans into gyral based regions of interest. Neuroimage, 31(3):968–980.

10. Fischl, B. (2012). FreeSurfer. Neuroimage, 62(2):774–781.

11. Mackey, S., Allgaier, N., Chaarani, B., Spechler, P., Orr, C., Bunn, J., Allen, N. B., Alia-Klein, N., Batalla, A., Blaine, S., et al. (2019). Mega-analysis of gray matter volume in substance dependence: general and substance-specific regional effects. American Journal of Psychiatry, 176(2):119–128.

12. Van Erp, T. G., Hibar, D. P., Rasmussen, J. M., Glahn, D. C., Pearlson, G. D., Andreassen, O. A., Agartz, I., Westlye, L. T., Haukvik, U. K., Dale, A. M., et al. (2016). Subcortical brain volume abnormalities in 2028 individuals with schizophrenia and 2540 healthy controls via the ENIGMA consortium. Molecular psychiatry, 21(4):547–553.

13. Van Erp, T. G., Walton, E., Hibar, D. P., Schmaal, L., Jiang, W., Glahn, D. C., Pearlson, G. D., Yao, N., Fukunaga, M., Hashimoto, R., et al. (2018). Cortical brain abnormalities in 4474 individuals with schizophrenia and 5098 control subjects via the enhancing neuro imaging genetics through meta analysis (ENIGMA) consortium. Biological psychiatry, 84(9):644–654.

14. Schmaal, L., Veltman, D. J., van Erp, T. G., Sämann, P., Frodl, T., Jahanshad, N., Loehrer, E., Tiemeier, H., Hofman, A., Niessen, W., et al. (2016). Subcortical brain alterations in major depressive disorder: findings from the ENIGMA Major Depressive Disorder working group. Molecular psychiatry, 21(6):806–812.

15. Schmaal, L., Hibar, D., Sämann, P. G., Hall, G., Baune, B., Jahanshad, N., Cheung, J., van Erp, T. G., Bos, D., Ikram, M. A., et al. (2017). Cortical abnormalities in adults and adolescents with major depression based on

brain scans from 20 cohorts worldwide in the ENIGMA Major Depressive Disorder Working Group. Molecular psychiatry, 22(6):900–909.

16. Groenewold, N. A., Bas-Hoogendam, J. M., Amod, A. R., Laansma, M. A., Van Velzen, L. S., Aghajani, M., Hilbert, K., Oh, H., Salas, R., Jackowski, A. P., et al. (2023). Volume of subcortical brain regions in social anxiety disorder: mega-analytic results from 37 samples in the ENIGMA-Anxiety Working Group. Molecular psychiatry, 28(3):1079–1089.